Eur. Phys. J. C 9, 283–312 (1999)
DOI 10.1007/s100529900044

THE EUROPEAN PHYSICAL JOURNAL C

Identification of the glueballs and the scalar meson nonet of lowest mass*

P. Minkowski[1], W. Ochs[2]

[1] Institute for Theoretical Physics, University of Bern, CH-3012 Bern, Switzerland
[2] Max Planck Institut für Physik, Werner Heisenberg Institut, D-80805 München, Germany

Received: 30 November 1998 / Revised version: 17 February 1999 / Published online: 27 April 1999

Abstract. We discuss the theoretical expectations and phenomenological evidence for the lightest glueballs and the members of the meson nonet with quantum numbers $J^{PC} = 0^{++}$. We reconsider the recent evidence for candidate states with masses below ∼1700 MeV, but include also the results from earlier phase-shift analyses. Arguments are presented to classify the scalars $f_0(980)$ and $f_0(1500)$ as members of the 0^{++} nonet, with a mixing rather similar to that of the pseudoscalars η' and η. The S-wave states called $f_0(400-1200)$ and $f_0(1370)$ are considered as different signals from a single broad resonance, which we take to be the lowest-lying 0^{++} glueball. This state together with $\eta(1440)$ and $f_J(1710)$ with spin $J = 2$ form the basic triplet of binary gluonic bound states. We argue that these hypotheses are consistent with what can be expected theoretically.

1 Introduction

An early prediction of QCD concerns the existence of a spectrum of glueballs, i.e. mesonic bound states of two or more constituent gluons, in addition to the spectrum of $q\overline{q}$ mesons with characteristic restrictions in the accessible quantum numbers [1]. Such glueball states have been searched for extensively. The first 20 years of searches have seen some interesting candidates [2], especially in gluon rich processes such as radiative J/ψ decays, but no clear and convincing evidence for the two kinds of spectroscopy have emerged, despite many efforts [3].

In the recent years these studies have entered a more optimistic phase. On one hand, the theoretical predictions from lattice QCD were claimed to become more accurate. For the purely gluonic theory these calculations put the lightest glueball into the mass region around 1600 MeV (for recent reviews, see [4,5]). On the other hand, there are new experimental investigations with high statistical precision aiming at a better understanding of the spectroscopy in the 1000-2000 MeV region, especially by the Crystal Barrel Collaboration [6–11] in the analysis of $p\overline{p}$ annihilation at rest and by the WA102 Collaboration [12, 13] studying central production in high energy pp collisions.

The analysis of the recent results with inclusion of certain older experimental data has apparently brought a new consensus supporting the lattice result with a $J^{PC} = 0^{++}$ glueball around 1600 MeV. In this channel more states are reported than are expected for the $q\overline{q}$ nonet [14]. Prime candidates for the lightest glueball are the $f_0(1500)$ and the $f_J(1710)$ with spin taken as $J = 0$. As the decay branching ratios of these states do not follow closely the expectations for a glueball it is proposed that these states and also the $f_0(1370)$ represent mixtures of the glueball with the members of the $J^{PC} = 0^{++}$ nonet. With this mixing scheme various experimental results can be described [15–17].

In this paper we begin with a discussion of the theoretical expectations in Sect. 2. In particular it is pointed out that the first results from unquenched lattice calculations show large effects from sea quarks with the tendency to decrease the glueball mass with decreasing quark mass. The spectral sum rules require a gluonic contribution at low mass around 1 GeV. We discuss possible mass patterns for the scalar $q\overline{q}$ states in a model with general QCD potential and explicit chiral symmetry breaking by quark masses.

A closer look at the real world reveals a surprisingly complex experimental situation and we implement the data with several *phenomenological hypotheses* :

a) Despite the eventually strong mixing between quark and gluon states it is possible to classify the "more" quark like states with $L_{q\bar{q}} = 1$ into four nonets.
b) The four isoscalar members of the respective nonets with largest mass do not exceed (by more than ∼100 MeV) the mass of $f_2'(1525)$.
c) All members of the four nonets in question have been observed, possibly with incorrect assignment of quantum numbers [18] .

In Sect. 3 we begin our phenomenological analysis and discuss in some detail the evidence for resonance states

* Work supported in part by the Schweizerischer Nationalfonds.

in the mass range below ∼1700 MeV. We pay particular attention to the earlier results from elastic and inelastic $\pi\pi$ scattering which allow in principle the determination of the amplitude phase. It is the evidence for the moving phase of the Breit-Wigner amplitude which is necessary to establish a resonant state. The restriction to the study of resonance peaks may become misleading, especially if the state is broad and above "background". The present analysis confirms the amplitude "circles" for the $f_0(1500)$ whereas we do not accept the $f_0(1370)$ listed by the Particle Data Group (PDG) [18] as a genuine resonant state.

In Sect. 4 we study the additional information provided by the various couplings in production and decay in order to identify the members of the $J^{PC} = 0^{++}$ nonet. The satisfactory solution includes the $f_0(980)$ and $f_0(1500)$. There is the broad object seen in $\pi\pi$ scattering, often called "background", which extends from about 400 MeV up to about 1700 MeV. This object we consider as a single broad resonance[1] which we identify as the lightest glueball with quantum numbers $J^{PC} = 0^{++}$ as will be discussed in Sect. 5. Two further states with $J^{PC} = 0^{-+}$ and $J^{PC} = 2^{++}$ complete the basic triplet of binary gluon states (Sect. 6).

The conclusions are drawn in Sect. 7, in particular, we compare our spectroscopic conclusions with the theoretical expectations.

2 Theoretical expectations

The purpose of this section is to clarify the possible mass patterns of the lightest mesons which are either bound states of quark-antiquark or of gluons. We assume the dynamics to be reducible to chromodynamics with three light flavors u, d and s.

2.1 Properties of low mass glueballs

2.1.1 Scenarios for glueball and $q\overline{q}$ spectroscopy

We consider first the spectroscopy in the chiral and antichiral limits

$$\begin{aligned} \chi_3 &: \lim\, m_{u,d,s} = 0 \\ \chi_2 &: \lim\, m_{u,d} = 0 \;\; ; \;\; m_s > 0 \\ \overline{\chi} &: \lim\, m_{u,d,s} \to \infty \end{aligned} \tag{1}$$

In the antichiral limit $\overline{\chi}$ the gluon states become separately visible. The quantum numbers of these states, scenarios for their masses as well as the decay properties have been discussed in [1]. Here we consider the basic triplet of binary glueball states gb_i which can be formed by two "constituent gluons" and correspond to the three invariants which can be built from the bilinear expression of gluon fields $F_a^{\mu\nu}F^{a\rho\sigma}$ with J^{PC} quantum numbers

$$gb_0(0^{++}), \quad gb_1(0^{-+}) \quad \text{and} \quad gb_2(2^{++}) \tag{2}$$

[1] we refer to it as "red dragon"

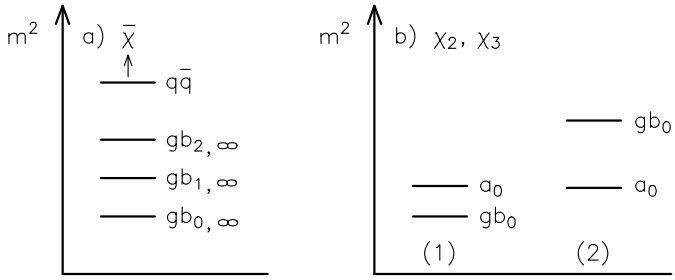

Fig. 1. Schematic representation of the mass spectra of glueballs and $q\overline{q}$ states in the antichiral limit $\overline{\chi}$ ($m_q \to \infty$) and in the chiral limits χ_2, χ_3 of (1)

corresponding to the helicity wave functions of the two "constituent gluons" $|11\rangle + |-1-1\rangle$, $|11\rangle - |-1-1\rangle$ and $|1-1\rangle$ (or $|-11\rangle$). Theoretical calculations to be discussed below (bag model, sum rules, lattice) suggest the 0^{++} state to be the lightest one

$$m_{gb_0} \;<\; m_{gb_1} \;,\; m_{gb_2} \tag{3}$$

and these three states dominate the low energy dynamics. In the antichiral limit $\overline{\chi}$ the mass $m_{gb_{0,\infty}}$ of the scalar glueball meson defines the mass gap in the purely gluonic world; in this limit at least the lightest scalar and pseudoscalar glueballs are stable.

In the chiral limits χ_2 and χ_3 the $q\overline{q}$ multiplets may partly overlap in mass with the glueball states. Of special interest is the multiplet with the quantum numbers of the vacuum 0^{++} as its members have the same quantum numbers as the glueball of lowest mass. We focus on the two alternatives for the glueball mass m_{gb_0} and the mass of the lightest particle $m_{a_0} \sim 980$ MeV of the scalar $q\overline{q}$ nonet (see Fig. 1)

1) $m_{gb_0} \lesssim m_{a_0}$ corresponding to a "light" glueball
2) $m_{gb_0} \gg m_{a_0}$ corresponding to a "heavy" glueball. This condition is considered to be met if m_{gb_0} exceeds ~ 1500 MeV.

The first alternative is an extension of scenario A, the second one of scenario(s) B(C) discussed in [1].

In case 2) the basic triplet of binary glueballs is in the high mass region. Then their width is expected to be small according to perturbative arguments ("gluonic Zweig rule" [1]). Also in this case the glueball states may be well separated in mass from the states in the $q\overline{q}$ nonet of lowest mass.

In case 1) which we favor the width of gb_0 could be large. First, the gluonic Zweig rule cannot be invoked any more as the coupling α_s at low energies may become large. Secondly, the main decay mode is the pseudoscalar channel $\pi\pi$ and at higher mass also $K\overline{K}$ and $\eta\eta$ and there is a dynamical argument based on the overlap of the wave functions between the external pseudoscalar states and the intermediate gluon states: The angular momentum between the constituent 2 gluons is dominated by S waves ($L_{gg} = 0$) and so are the open pseudoscalar decay channels such as $\pi\pi$. This alignment of S wave dominance in constituent quanta and two body decay channels distin-

guishes gb_0 from the 0^{++} $q\overline{q}$ states which form an intermediate P-wave. The same is also true for the lowest $q\overline{q}$ vector mesons where the intermediate S wave contrasts with the external P waves. We therefore expect

$$\Gamma_{gb_0} \gg \Gamma_{q\overline{q}-hadron}. \quad (4)$$

Both arguments, the large coupling and the large overlap of internal and external wave functions lead to the expectation of a broad 0^{++} glueball if it is light.

2.1.2 Bag models

A dynamical calculation of hadron masses has been achieved in models where quarks and massless gluons are confined in spherical bags of similar size. If the gg interaction is neglected one expects [19] the lightest glueball states with even parity to be degenerate in mass and the same holds for the states with odd parity:

$$\begin{aligned} \alpha_s = 0: \quad & m_{gb}(0^{++}) \sim m_{gb}(2^{++}) \sim 0.87 \text{ GeV} \\ & m_{gb}(0^{-+}) \sim m_{gb}(2^{-+}) \sim 1.3 \text{ GeV} \end{aligned} \quad (5)$$

Inclusion of the gg interaction leads to a hyperfine splitting and typically a mass ordering [2]

$$\alpha_s \neq 0: \qquad m_{gb_0} < m_{gb_1} < m_{gb_2}. \quad (6)$$

The energy shifts in $O(\alpha_s)$ are calculated [20] in terms of two parameters, the coupling α_s and the cavity radius a. Reasonable values for these parameters consistent with $q\overline{q}$ spectroscopy ($\alpha_s = 0.748$, $a^{-1} = 0.218$ GeV) led to an identification of the 0^{-+} glueball with $\eta(1440)$ and of 2^{++} with $f_J(1720)$ in today's nomenclature. The mass for the 0^{++} glueball was then *predicted* as

$$m_{gb_0} \sim 1 \text{ GeV}. \quad (7)$$

and because of the self energy of the gluons in the bag this mass can hardly become smaller. So in this unified treatment of $q\overline{q}$ and gluonium spectroscopy the "light glueball" scenario 1) is preferrred.

2.1.3 QCD Spectral sum rules

In a recent application of the sum rule approach [21] the basic quadratic gauge boson bilinear operators with quantum numbers $J^{PC} = 0^{++}$, 0^{-+} and 2^{++} have been analysed by Narison [22] together with the lowest quark antiquark operators. Constraints for the masses of a sequence of states are obtained by saturating the spectral sum rules. It is interesting to note that in the 0^{++} channel not all sum rules can be satisfied by a single glueball at a mass of around 1500 MeV – as suggested by quenched lattice calculations. Rather one is forced to include contributions from lower mass around 1 GeV with a large width. A consistent solution is found with two states $\sigma_B(1000), \sigma'_B(1370)$ which both have large gluonic couplings. A sum rule fit which includes a light glueball with mass around 500 MeV besides a heavier one at 1700 MeV has been presented by Bagan and Steele [23]. We take these results as a further hint towards the need of a light glueball in agreement with our findings.

On the other hand, the spectrum of the next heavier gluon states differs from our suggestions. Also our assignment of the scalar $q\overline{q}$ nonet is different from the one in [22] and not along the OZI rule.

Table 1. Assignment of the (bare) scalar $\overline{q}q$ nonet according to Weingarten [25]

name	$\overline{q}q$	mass^2 [GeV^2]	mass [GeV]
$f_0(1390)$	$\frac{1}{\sqrt{2}}(\overline{u}u + \overline{d}d)$	1.932	1.390
$a_0^0(1450)$	$\frac{1}{\sqrt{2}}(\overline{u}u - \overline{d}d)$	2.102	1.450
$K_0^*(1430)$	$\overline{s}q,\ s\overline{q}$	2.042	1.429
$f_0(1500)$	$\overline{s}s$	2.265	1.505

2.1.4 Results from lattice gauge theory

A serious tool to assess the spectral location of glueball states – in particular in the antichiral limit, where all quark masses are sent to infinity – comes from simulations of pure $SU(3)_c$ Yang Mills theories on a lattice [24–26]. First results from full QCD including sea quarks became available recently [27,28].

In the calculations without quarks one finds the lowest lying scalar glueball gb_0 in the mass range 1500 - 1700 MeV which corresponds to our high mass scenario 2) discussed above. In the scenario suggested by Weingarten [25] the members of the scalar $q\overline{q}$ nonet are taken to be the observed states listed in Table 1. The quark composition is assumed along the OZI rule. The actually observed particles with 0^{++} quantum numbers $a_0(980)$ and $f_0(980)$ at lower energies are considered as "irrelevant to glueball spectroscopy" and not taken as candidates for the scalar nonet. In a variant of this phenomenological scheme [15,5, 25] one includes the $f_J(1720)$ with spin assignment $J = 0$ and assumes the three observed 0^{++} states to be a superposition of the bare glueball and the two bare isoscalar $q\overline{q}$ states. In this mixing scheme one can take into account the observed small $K\overline{K}$ branching ratio of the $f_0(1500)$.

First calculations in unquenched QCD including two flavors of quark have been carried out by Bali et al. [27, 28]. Results from a $16^3 \times 32$ lattice with an inverse lattice spacing of $2 - 2.3$ GeV show a definite dependence of the results on the quark mass and correspondingly on the pion mass. If the pion mass is lowered from about 1000 to 700 MeV the 0^{++} glueball mass decreases from 1400 to about 1200 MeV (using the data in [28]). The quark masses are still quite large but in any case the glueball mass becomes smaller than in case of the quenched approximation without quarks (see Table 2). On the other hand, the calculations [28] also indicate a significant dependence on the volume. For a $24^3 \times 40$ lattice the glueball mass goes up again to the larger number of the quenched calculation.

Table 2. Glueball masses with statistical and systematic errors in quenched lattice approximation whereby the first two determinations are based on data in [24] (upper part) and with inclusion of sea quarks for different spatial lattice sizes L_S (lower part)

author	m_{gb_0} [MeV]	n_{fl}	m_π [MeV]
Teper [5]	$1610 \pm 70 \pm 130$	0	
Weingarten [25]	1707 ± 64	0	
Morningstar et al. [26]	$1630 \pm 60 \pm 80$	0	
Bali et al. [27,28]	~ 1200 ($L_S = 16$)	2	$700 - 1000$
Bali et al. [28]	~ 1700 ($L_S = 24$)	2	

Table 3. The ratio R of the a_0-mass and the string tension as function of the square of the lattice spacing a in units of the string tension. The last column shows the ratio R multiplied with the physical value of the string tension 0.427 GeV [29]

β	a^2/K	$R = aM_{a0}/a\sqrt{K}$	$R\sqrt{K}$ [GeV]
6.0	0.048	3.72 ± 0.15	1.59 ± 0.06
6.2	0.026	2.86 ± 0.13	1.22 ± 0.05

We conclude from the mass values in Table 2 that the quenched calculation supports the "high mass region" for the lightest glueball, i.e. our alternative 2), while the results with sea quarks do not exlude the opposite, i.e. gb_0 placed into the "low mass region", in view of the large values of the quark masses in the calculation and the observed decrease of the glueball mass with the quark mass.

It is also of great interest to compute the mass of the lightest scalar state $a_0(0^{++})$ in lattice QCD. First results have been obtained recently in quenched approximation with non-perturbatively $O(a)$ improved Wilson fermions [29] for two values of the coupling β, see Table 3.

The ratio $R\sqrt{K}$ in the last column of Table 3 extrapolates to the physical mass in the continuum limit $a^2 \to 0$. As can be seen these mass values decrease in the approach of this limit, the lowest mass value being $M_{a_0} \sim 1.2$ GeV. A reliable extrapolation from two data points cannot be expected. If one extrapolates nevertheless one finds $M_{a_0} \sim 0.8$ GeV. These results seem to be consistent with the mass 0.98 GeV for the lightest scalar meson, but the heavier mass 1.45 GeV as suggested for this state by Weingarten cannot be excluded on the basis of only two measurements.[2] With improved accuracy such calculations could provide an interesting hint towards the classification of the $a_0(980)$ state as the lowest mass scalar meson.

The results reported here indicate that our hypothesis of a light glueball with mass around 1 GeV accompanied by a scalar nonet with particles around 1 GeV is not necessarily in contradiction with lattice QCD results. We also wish to point out that the parametrization of the 0^{++} spectrum in terms of one resonance only may not be appropriate; this was found in case of QCD sum rules and may be true in particular if the lightest state is very broad.

[2] We thank D. Pleiter and S. Aoki for helpful discussions of these results

2.2 The scalar nonet and effective Σ variables

An important precondition for the assignment of glueball states is the understanding of the low mass $q\bar{q}$ spectroscopy. As the lightest glueball is expected with $J^{PC} = 0^{++}$ quantum numbers we focus here on the expectations for the lightest scalar $q\bar{q}$ nonet. The lightest particles with these quantum numbers are $a_0(980)$ and $f_0(980)$, approximately degenerate in mass. Some authors consider one or both of these states as $K\overline{K}$ molecules [30] and take $a_0(1450)$ and $f_0(1370)$ (or a broad $f_0(1000)$) as members of the scalar nonet. The next (uncontroversial) candidate for the nonet is $K_0^*(1430)$; the last member of the nonet is a heavier isoscalar state $f_{0>}$, possibly $f_0(1500)$ or $f_J(1720)$, which can mix with the lighter $f_0(980)$.

An attractive theoretical approach to the scalar and pseudoscalar mesons is based on the "linear sigma models" which realize the spontaneous chiral symmetry breakdown (for reviews, see [31]). The requirement of renormalizability provides a considerable restriction in the functional form of the effective potential compared to what would be generally allowed. In a recent application Törnqvist [32] considered a renormalizable Lagrangian for the scalar and pseudoscalar sector. In his solution for the scalar nonet the OZI rule holds exactly for the bare states with a broad isoscalar non-strange "σ" resonance below 1 GeV and the $f_0(980)$ as the lowest $s\bar{s}$ state. The resulting mass spectrum, however, is considerably modified by unitarisation effects.

In an alternative approach [33–35] one starts from a 3-flavor Nambu-Jona-Lasinio model but includes an effective action for the sigma fields with an instanton induced axial $U(1)$ symmetry-breaking determinant term (proportional to I_3 in (11) below), along the suggestion by t'Hooft [36], which keeps the Lagrangian renormalizable. This corresponds again to a linear sigma model but now the scalars are close to the singlet and octet states, and they do not split according to the OZI rule; the sign of the mass splitting in the scalar and pseudoscalar sectors is reversed. This suggests $f_0(1500)$ to be near the octet state whereas different options are pursued for the lighter isoscalar f_0 and the isovector a_0 by the authors [33–35].

In our approach we do not follow the $K\overline{K}$ molecule hypothesis for the $f_0(980)$ and the $a_0(980)$ (see also the remarks in the next section) but take them as genuine members of the $q\bar{q}$ scalar nonet. In the rest of this section we discuss what can be derived about the mass of $f_{0>}$ and the mixing pattern in the scalar nonet from the most general effective QCD potential for the Σ-variables pertaining to the scalar and pseudoscalar mesons, whereby we do not restrict the analysis to renormalizable interaction terms. In this way we explore the consequences of chiral symmetry in the different limits in (1) in a general QCD framework.

Thereafter we turn to the phenomenological analysis of data where we try to minimize the theoretical preconditions as suggested by the present section.

2.2.1 Σ variables and chiral invariants

We assume that the glueball states do not affect in an essential way the remaining effective degrees of freedom at low energy. Then all degrees of freedom can be integrated out. The variables are those of a linear sigma model

$$\begin{aligned} \Sigma_{st} &= (\sigma_{st} - i\, p_{st}) \\ \sum_c \bar{q}^{\,c}_s q^{\,c}_t &\leftrightarrow \sigma_{st} \quad ; \quad \sum_c \bar{q}^{\,c}_s\, i\gamma_5\, q^{\,c}_t \leftrightarrow p_{st} \end{aligned} \tag{8}$$

where the indices s, t refer to the flavors u, d, s. We do not require interactions to be renormalizable, rather we study the general effective action of QCD restricted to the sigma variables [37]. The resulting mass spectra and mixings are then less restricted than in the renormalizable Lagrangian models: for example, OZI splitting is possible but not particularly favored.

In (8) we chose the normalization of the complex (non-hermitian) field variables Σ_{st} such that in the chiral limit χ_3 ($\lim m_{u,d,s} = 0$) the vacuum expected value corresponds to the (real) unit matrix :

$$\chi_3 \quad : \quad \langle \Omega \mid \Sigma_{st}(x) \mid \Omega \rangle \rightarrow \delta_{st}. \tag{9}$$

We propose to discuss the *general* form of the effective potential, more precisely its real part – restricted only to the first order approximation with respect to the strange quark mass term in the two flavor chiral limit χ_2 ($\lim m_{u,d} = 0$)

$$\begin{aligned} &\chi_2 : V(\Sigma) \rightarrow V_0 - \mu_s \,\mathrm{Re}\,\Sigma_{33}\,; \\ &\mu_s \propto m_s. \end{aligned} \tag{10}$$

The quark mass parameter μ_s in (10) is to be expressed in appropriate units (mass^4). V_0 refers to the chiral limit χ_3; it depends in an a priori arbitrary way on four base variables for which we can choose

$$\begin{aligned} I_1 &= \mathrm{tr}\,\Sigma\,\Sigma^\dagger - \mathrm{tr}\,\mathbf{1} \quad ; \\ I_2 &= \mathrm{tr}\,(\Sigma\,\Sigma^\dagger)^2 - \mathrm{tr}\,\mathbf{1} \\ I_3 &= \mathrm{Re\ Det}\,\Sigma - 1 \quad ; \\ I_4 &= \mathrm{Im\ Det}\,\Sigma \end{aligned} \tag{11}$$

If we introduce the shifted variables

$$\Sigma = \mathbf{1} + Z \quad ; \quad Z = s - i\,p \tag{12}$$

we can express the four invariants defined in (11) as

$$\begin{aligned} I_1 &= 2\,\mathrm{tr}\,s + \mathrm{tr}\,s^2 + \mathrm{tr}\,p^2 \\ I_2 &= 4\,\mathrm{tr}\,s + 6\,\mathrm{tr}\,s^2 + 2\,\mathrm{tr}\,p^2 \\ &\quad + 4\,\mathrm{tr}\,s^3 + 4\,\mathrm{tr}\,s\,p^2 \\ &\quad + \mathrm{tr}\,(Z\,Z^\dagger)^2 \\ I_3 &= \mathrm{tr}\,s + \tfrac{1}{2}\big((\mathrm{tr}\,s)^2 - \mathrm{tr}\,s^2 \\ &\quad - (\mathrm{tr}\,p)^2 + \mathrm{tr}\,p^2\big) \\ &\quad + \mathrm{Re}\,\tfrac{1}{6}\big((\mathrm{tr}\,Z)^3 \\ &\quad - 3\,\mathrm{tr}\,Z\,\mathrm{tr}\,Z^2 + 2\,\mathrm{tr}\,Z^3\big) \\ I_4 &= -\mathrm{tr}\,p - (\mathrm{tr}\,s\,\mathrm{tr}\,p - \mathrm{tr}\,s\,p) \\ &\quad + \mathrm{Im}\,\tfrac{1}{6}\big((\mathrm{tr}\,Z)^3 - 3\,\mathrm{tr}\,Z\,\mathrm{tr}\,Z^2 \\ &\quad + 2\,\mathrm{tr}\,Z^3\big) \end{aligned} \tag{13}$$

There is no loss of generality - *concentrating on scalar mass terms only* - to restrict Σ to the hermitian matrix s whereby the four variables in (11) reduce to three:

$$\begin{aligned} I_1 &\rightarrow 2\,\mathrm{tr}\,s + \mathrm{tr}\,s^2 \\ I_2 &\rightarrow 4\,\mathrm{tr}\,s + 6\,\mathrm{tr}\,s^2 + 4\,\mathrm{tr}\,s^3 + \mathrm{tr}\,s^4 \\ I_3 &\rightarrow \mathrm{tr}\,s + \tfrac{1}{2}\big((\mathrm{tr}\,s)^2 - \mathrm{tr}\,s^2\big) \\ &\quad + \tfrac{1}{6}\big((\mathrm{tr}\,s)^3 - 3\,\mathrm{tr}\,s\,\mathrm{tr}\,s^2 \\ &\quad + 2\,\mathrm{tr}\,s^3\big). \end{aligned} \tag{14}$$

2.2.2 Scalar mass terms to order μ_s

To the precision required we need the expansion of $V_0(s)$ to third order in the matrix variable s. To third order in s the three base variables in (14) can be replaced by the simple power basis $\mathrm{tr}\,s$, $\mathrm{tr}\,s^2$, $\mathrm{tr}\,s^3$. As a consequence $V_0(s)$ is of the form

$$\begin{aligned} V_0 &= \tfrac{1}{2}\big(A\,\mathrm{tr}\,s^2 + B(\mathrm{tr}\,s)^2\big) + \\ &\quad \tfrac{1}{3}C\,\mathrm{tr}\,s^3 + \tfrac{1}{2}D(\mathrm{tr}\,s)\,\mathrm{tr}\,s^2 + \\ &\quad \tfrac{1}{3}E(\mathrm{tr}\,s)^3 + O(s^4). \end{aligned} \tag{15}$$

We shall neglect the terms of order s^4 in the following. To first order in the strange quark mass the vacuum expected

values are shifted from their values in (9) according to (10)

$$\langle\, \Omega \mid \Sigma \mid \Omega \,\rangle \;=\; \mathbf{1} \;+\; \langle\, s \,\rangle \quad ; \quad s \;=\; \langle\, s \,\rangle \;+\; x$$

$$A\, \langle\, s \,\rangle \;+\; B\, \mathrm{tr}\, \langle\, s \,\rangle\, \mathbf{1} \;=\; \mu_{\,s}\, P_3 \quad ;$$

$$P_3 \;=\; \begin{pmatrix} 0\,0\,0 \\ 0\,0\,0 \\ 0\,0\,1 \end{pmatrix} \tag{16}$$

$$\langle\, s \,\rangle \;=\; \frac{\mu_s}{A} \left(P_3 \;-\; \frac{B}{A+3B}\, \mathbf{1} \right)$$

Thus the quadratic parts with respect to x of V to first order in the strange quark mass are of the form

$$\begin{aligned} V^{\,(2)} \;=\; & \tfrac{1}{2} \left(A\, \mathrm{tr}\, x^{\,2} \;+\; B\, (\, \mathrm{tr}\, x \,)^{\,2} \right) \;+ \\ & C\, \mathrm{tr}\, \langle\, s \,\rangle\, x^{\,2} \;+\; D\, (\, \mathrm{tr}\, x \,)\, \mathrm{tr}\, \langle\, s \,\rangle\, x \;+ \\ & \tfrac{1}{2}\, D\, (\, \mathrm{tr}\, \langle\, s \,\rangle \,)\, \mathrm{tr}\, x^{\,2} \;+ \\ & E\, (\, \mathrm{tr}\, \langle\, s \,\rangle \,)\, (\, \mathrm{tr}\, x \,)^{\,2}. \end{aligned} \tag{17}$$

The first two terms composing $V^{\,(2)}$ in (17) describe singlet and octet masses (squares) $m_{\,(1)}$ and $m_{\,(8)}$ in the u-d-s chiral limit χ_3 , whereas the remaining terms contain the further mass splittings to first order in the strange quark mass. Introducing the quantities

$$m^{\,2}_{\,(1)} = \; A \;+\; 3\, B \quad ; \qquad m^{\,2}_{\,(8)} = \; A$$

$$R = \; \frac{m^{\,2}_{\,(8)}}{m^{\,2}_{\,(1)}} \; ; \qquad (\, c \,,\, d \,,\, e \,) = \; \frac{\mu_s}{A}\, (\, C \,,\, D \,,\, E \,) \tag{18}$$

the expression for $V^{\,(2)}$ in (17) becomes

$$\begin{aligned} V^{\,(2)} \;=\; & \left[\, A \;+\; \tfrac{2}{3}\, c\, (\, R \;-\; 1 \,) \;+\; d\, R \,\right] \tfrac{1}{2}\, \mathrm{tr}\, x^{\,2} \\ & +\left[\, B \;+\; \tfrac{2}{3}\, d\, (\, R \;-\; 1 \,) \right. \\ & \left. +\; 2\, e\, R \,\right] \tfrac{1}{2}\, (\, \mathrm{tr}\, x \,)^{\,2} \\ & +c\, \mathrm{tr}\, P_3\, x^{\,2} \;+\; d\, (\, \mathrm{tr}\, x \,)\, \mathrm{tr}\, P_3\, x. \end{aligned} \tag{19}$$

Remark on the (semi)classical interpretation of $V^{\,(2)}$

We assume here and in the following that the (semi)-classical interpretation of $V^{\,(2)}\, (\, x \,)$ as a quadratic function of the shifted field variables x actually describes the real part of the mass (square) term pertaining to scalar mesons and can be extended to pseudoscalar mesons, while we neglect the specific $m_{\,s}$ dependence of the kinetic energy term, which within the same (semi)classical interpretation is in general simplified to remain unperturbed, i.e. of the form

$$\mathcal{L}_{\,kin} \;=\; \tfrac{1}{4}\, f_{\,\pi}^{\,2}\, \mathrm{tr}\, \left(\, \partial^{\,\varrho}\, \Sigma^{\,\dagger}\, \partial_{\,\varrho}\, \Sigma \,\right). \tag{20}$$

In (20) $f_{\,\pi} \;\sim\; 93$ MeV denotes the pseudoscalar decay constant in the three flavor chiral limit.

The simplified form of the kinetic energy term in (20) can always be achieved after a nonlinear transformation of the Σ variables. The corresponding chiral (Noether) currents are then only proportional to the respective quark bilinear currents modulo explicitely $m_{\,s}$ dependent factors as visible in the ratio of physical pion to kaon decay constants, far away from the flavor symmetric limit 1.

2.2.3 Mass square patterns for the scalar nonet

It follows from the structure of the mass terms in (19) that the (nearly perfect) degeneracy of the f_0 (980) and a_0 (980) isosinglet and isotriplet levels can only be realized independently of $m_{\,s}$ if the constant B prevailing in the $\chi_{\,3}$ limit vanishes. We adopt thus $B \;=\; 0$ in the following, which implies that the entire scalar nonet is degenerate in mass in the chiral limit $\chi_{\,3}$. Thus the expression for $V^{\,(2)}$ in (19) becomes

$$\begin{aligned} V^{\,(2)} \;=\; & [\; A \;+\; d \,]\; \tfrac{1}{2}\, \mathrm{tr}\, x^{\,2} \;+\; e\, (\, \mathrm{tr}\, x \,)^{\,2} \;+ \\ & c\, \mathrm{tr}\, P_3\, x^{\,2} \;+\; d\, (\, \mathrm{tr}\, x \,)\, \mathrm{tr}\, P_3\, x. \end{aligned} \tag{21}$$

The first term on the right hand side of (21) yields a common mass square to the entire nonet. Hence, if we consider all mass squares relative to $m^{\,2}\, (\, a_0 \,)$ all contributions are contained in the last three terms composing $V^{\,(2)}$, which we denote by $\Delta\, m^{\,2} \;=\; m^{\,2} \;-\; m^{\,2}\, (\, a_0 \,)$

$$\begin{aligned} \Delta\, m^{\,2} \;=\; & c\, \mathrm{tr}\, P_3\, x^{\,2} \;+\; d\, (\, \mathrm{tr}\, x \,)\, \mathrm{tr}\, P_3\, x \\ & +\, e\, (\, \mathrm{tr}\, x \,)^{\,2} \\ \mathrm{tr}\, P_3\, x^{\,2} \;=\; & \overline{K}\, K \;+\; \tfrac{2}{3}\, S^{\,2}_{\,(8)} \;-\; 2\, \tfrac{\sqrt{2}}{3}\, S_{\,(8)}\, S_{\,(1)} \\ & +\, \tfrac{1}{3}\, S^{\,2}_{\,(1)} \\ (\, \mathrm{tr}\, x \,)\, \mathrm{tr}\, P_3\, x \;=\; & -\, 2\, \tfrac{1}{\sqrt{2}}\, S_{\,(8)}\, S_{\,(1)} \;+\; S^{\,2}_{\,(1)} \\ (\, \mathrm{tr}\, x \,)^{\,2} \;=\; & 3\, S^{\,2}_{\,(8)}. \end{aligned} \tag{22}$$

In (22) $S_{\,(1)}$, $S_{\,(8)}$ denote the (hermitian) singlet, octet component fields within the scalar nonet respectively. Furthermore

$$x_{\,33} \;=\; \tfrac{1}{\sqrt{3}}\, S_{\,(1)} \;-\; \tfrac{2}{\sqrt{6}}\, S_{\,(8)}. \tag{23}$$

From the structure of $\Delta\, m^{\,2}$ in (22) we obtain the mass of the $K\, \overline{K}$ system

$$\Delta\, m^{\,2}\, (\, K \,) \;=\; c \tag{24}$$

as well as the mass and mixing pattern involving the two isosinglets $S_{\,(1)}$ and $S_{\,(8)}$. We introduce the octet-singlet

mixing matrix $\Delta\, m^{\,2}_{8-1} \equiv \Delta\, M^{\,2}$, which generates the quadratic form in $S_{(8)}$, $S_{(1)}$ in (22)

$$\Delta\, M^{\,2} = \begin{pmatrix} \frac{4}{3}\, c & -\sqrt{2}\ \left(\frac{2}{3}\, c + d\right) \\ -\sqrt{2}\ \left(\frac{2}{3}\, c + d\right) & \frac{2}{3}\, c + 2\, d + 6\, e \end{pmatrix} \tag{25}$$

which we can transform into

$$\Delta\, M^{\,2} = \tfrac{4}{3} c \begin{pmatrix} 1 & -\frac{1}{\sqrt{2}}(1+\delta) \\ -\frac{1}{\sqrt{2}}(1+\delta) & \frac{1}{2}\left((1+\delta)^2 + \varepsilon - \delta^2\right) \end{pmatrix}$$

$$\delta = \tfrac{3}{2}\tfrac{d}{c}\,; \quad \varepsilon = \tfrac{9\, e}{c}\,;$$

$$\mathrm{Det}\ \Delta\, M^{\,2} = \tfrac{8}{9}\, c^{\,2}\,(\,\varepsilon - \delta^{\,2}\,). \tag{26}$$

The mass square differences of the lighter and heavier isoscalar $f_{0<}$, $f_{0>}$ are obtained as eigenvalues of $\Delta\, M^{\,2}$. We note that the observed (approximate) degeneracy of $f_0\,(980)$ and $a_0\,(980)$, i.e. $\Delta\, m\,(\,f_{0<}\,) \sim 0$, corresponds through first order in $m_{\,s}$ to the vanishing determinant of $\Delta\, M^{\,2}$

$$\mathrm{Det}\ \Delta\, M^{\,2} = 0 \quad \leftrightarrow \quad \varepsilon = \delta^{\,2}$$

$$\Delta\, M^{\,2} = \tfrac{4}{3}\, c \begin{pmatrix} 1 & k \\ k & k^{\,2} \end{pmatrix} \quad ; \quad k = -\,\tfrac{1}{\sqrt{2}}\,(\,1 + \delta\,). \tag{27}$$

Introducing the mixing angle Θ by

$$\begin{aligned} f_{0>} &= \cos\,\Theta\, S_{(8)} + \sin\,\Theta\, S_{(1)} \\ f_{0<} &= -\,\sin\,\Theta\, S_{(8)} + \cos\,\Theta\, S_{(1)} \end{aligned} \tag{28}$$

we find the mass square and mixing pattern due to $\Delta\, M^{\,2}$ in (27), with $k = \tan\Theta$, to be given by

$$\Delta\, m^{\,2}\,(\,f_{0>}\,) = \frac{4}{3}\, c\, \frac{1}{\cos^2\,\Theta}\,; \quad \Delta\, m^{\,2}\,(\,f_{0<}\,) = 0. \tag{29}$$

Note that in the present approximation there is the inequality

$$\Delta\, m^{\,2}\,(\,f_{0>}\,) > \frac{4}{3}\, \Delta\, m^{\,2}\,(\,K\,). \tag{30}$$

Finally, we consider two limiting patterns for the mass square of scalar mesons :

I) No or small singlet octet mixing.
a) No mixing:
This assignment corresponds to

$$k = 0 \quad ; \quad \delta = -\,1 \quad ; \quad d = -\,\tfrac{2}{3}\, c. \tag{31}$$

In the following discussion we use as unit of mass square the $K_0^* - a_0$ splitting constant c in (24) and denote the common nonet mass in the $\chi_{\,3}$ limit by $m_{\,(9)}$. Relative to $m^{\,2}_{(9)}$ the four degenerate states $f_{0<}$, a_0 are lower in mass square by $\frac{2}{3}$ units, the K_0^*, $\overline{K_0^*}$ states are higher by $\frac{1}{3}$ unit, whereas $f_{0>}$ is raised by $\frac{2}{3}$ units. To first order in m_s the Gell-Mann-Okubo mass square formula is valid within the octet

$$3\, \Delta\, m^{\,2}\,(\,f_{0>}\,) = 4\, \Delta\, m^{\,2}\,(\,K_0^*\,) \tag{32}$$

and yields a prediction for the mass of the heavier isoscalar

$$m\,(\,f_{0>}\,) \sim 1550\ \mathrm{MeV}. \tag{33}$$

This mass pattern is also displayed in Fig. 2 (Ia) together with the one for the pseudoscalars for comparison. According to (30) the mass value (33) is the lower limit for $m(f_{0>})$ under the condition $m(a_0) = m(f_{0<})$.

b) Small mixing as in the pseudoscalar nonet
This mixing pattern is suggested by our phenomenological analysis in the following sections and corresponds to

$$\begin{aligned} k = \tfrac{1}{\sqrt{8}} \quad ; \quad \Theta &= \arcsin\,\tfrac{1}{3} \sim 19.5^{\mathrm{o}} \\ \Delta\, m^{\,2}\,(\,f_{0>}\,) = \tfrac{3}{2}\, \Delta\, m^{\,2}\,(\,K_0^*\,) \quad &\rightarrow \quad m\,(\,f_{0>}\,) \\ &\sim 1600\ \mathrm{MeV}. \end{aligned} \tag{34}$$

Relative to $m^{\,2}_{(9)}$ the four degenerate states $f_{0<}$, a_0 are now lower in mass square by one unit, the K_0^*, $\overline{K_0^*}$ states are at the same level, whereas $f_{0>}$ is raised by $\frac{1}{2}$ units (see Fig. 2).

II) Strict validity of the OZI rule.
Flavor mixing according to the OZI-rule corresponds to $\delta = 0$ and thus to

$$\begin{aligned} k = -\,\tfrac{1}{\sqrt{2}} \quad ; \quad \Theta &= -\,\arcsin\,\tfrac{1}{\sqrt{3}} \sim -\,35.3^{\mathrm{o}} \\ \Delta\, m^{\,2}\,(\,f_{0>}\,) = 2\, \Delta\, m^{\,2}\,(\,K_0^*\,) \quad &\rightarrow \quad m\,(\,f_{0>}\,) \\ &\sim 1770\ \mathrm{MeV}. \end{aligned} \tag{35}$$

In this case the four degenerate states $f_{0<}$, a_0 remain at the same level as $m^{\,2}_{(9)}$, the K_0^*, $\overline{K_0^*}$ states are higher by one unit, whereas $f_{0>}$ is raised by two units (see Fig. 2).

We conclude that the degeneracy in mass of $f_0(980)$ and $a_0(980)$ indeed implies a full degenerate nonet in the $\chi_{\,3}$ chiral limit. It is important to note, however, that the contributions of order m_s can respect the $f_0 - a_0$ mass degeneracy, without splitting necessarily the nonet according to the OZI-rule, i.e. according to flavor, as often assumed. Furthermore we point out, that an eventual similarity of

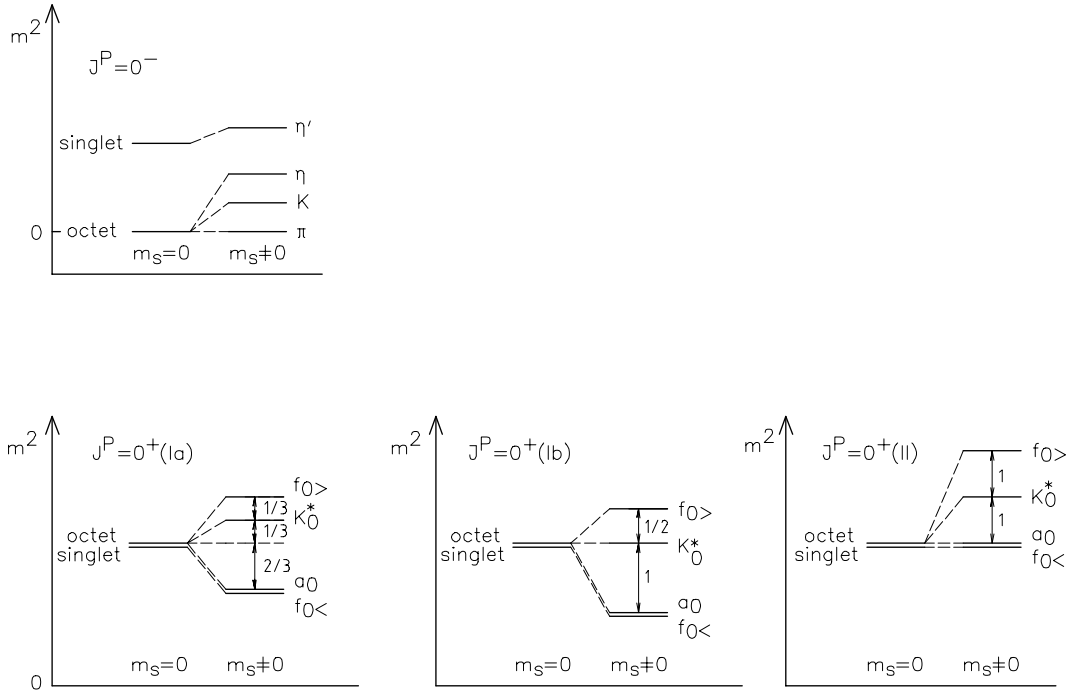

Fig. 2. Mass splitting of the pseudoscalar states in the chiral limit χ_3 with all $m_q = 0$ and after the strange quark mass m_s is set nonzero, and the same for the scalar states for three different choices of the singlet octet mixing angle: Ia) mixing angle $\Theta = 0$ (no mixing), Ib) small mixing angle $\Theta = \arcsin \frac{1}{3}$ (as for pseudoscalars), and II) mixing angle $\Theta = -\arcsin \frac{1}{\sqrt{3}}$ (according to OZI-rule)

singlet octet mixing for scalars *and* pseudoscalars as outlined in Ib) is by no means excluded. Approximate singlet-octet mixing is known to prevail for the latter – with a mixing angle near 19.5° as in (34) [38].

Only case I) is compatible with our phenomenological analysis in the subsequent sections and we assign

$$f_{0\,>} \;\rightarrow\; f_0(1500). \tag{36}$$

The observed mass is slightly lower than the masses theoretically calculated in the lowest order of the strange quark mass m_s. We emphasize here, that the splitting between a_0 and K_0^* is considerable and thus there will be non-negligible corrections of higher order in m_s, in particular to the K_0^*, $\overline{K_0^*}$ square masses. These corrections can easily account for the violation of the inequality (30) and the larger $f_{0\,>}$ masses predicted.

The alternative choice II would treat $f_0(980)$ as purely nonstrange state which is not attractive phenomenologically as will be discussed below. The pure $s\overline{s}$ state $f_{0\,>}$ with mass as in (35) could then be associated with the $J = 0$ component of $f_J(1710)$ (see, Sect. 6) but not much is known about the flavor properties of this state. In any case, the mass ordering of the three spin triplet states

$$f_{\,J\to 0}\,(1710) \quad ; \quad f_{\,1}\,(1510) \quad ; \quad f_{\,2}^{\,\prime}\,(1525) \tag{37}$$

would be upset by $\sim$ 200 MeV within this scheme.

3 Spectroscopy of light isoscalar $J^{PC} = 0^{++}$ states

Next we turn to the more detailed phenomenological discussion, first concerning the lowest mass $q\overline{q}$ nonet and the lightest glueball. Much effort has been devoted to clarify the experimental situation. To this end a variety of reactions has been studied in considerable detail

$$\begin{aligned}
&1.\ \pi^+\pi^- \to \pi^+\pi^-,\ \pi^0\pi^0\\
&2.\ \pi^+\pi^- \to K^+K^-,\ K^0\overline{K^0}\\
&3.\ \pi^+\pi^- \to \eta\eta,\ \eta\eta'\\
&4.\ p\overline{p} \to 3\pi^0,\ 5\pi^0,\ \pi^0\pi^0\eta,\ \eta\eta\pi^0, \eta\eta'\pi^0\\
&5.\ J/\psi \to \phi\pi\pi,\ \phi K\overline{K},\ \omega\pi\pi,\ \omega K\overline{K}\\
&6.\ J/\psi \to \gamma\pi\pi,\ \gamma K\overline{K},\ \gamma\eta\eta,\ \gamma\eta\eta'\\
&7.\ pp \to pp\ +\ X_{\rm central}\\
&8.\ \psi' \to J/\psi\pi\pi,\ Y' \to Y\pi\pi,\ Y'' \to Y\pi\pi\\
&9.\ \gamma\gamma \to \pi\pi,\ K\overline{K}
\end{aligned} \tag{38}$$

Our knowledge about the first three reactions comes from the analysis of peripheral πN collisions in application of the one-pion-exchange model; these reactions represent the oldest source of information on the scalar resonances. The fourth one, $p\overline{p}$ annihilation at threshold, has been studied in recent years with high statistics at the LEAR facility at CERN and has improved our understanding of the spectroscopy above 1 GeV in particular; data from higher primary energies have been obtained at FERMILAB. The states recoiling against the ϕ and the ω in

reaction 5 should have a large strange or nonstrange $q\overline{q}$ component respectively. The reactions 6,7 and 8 are expected to provide a gluon rich environment favorable for glueball production (for a review, see [2]), whereas in the last one (9) the glueball production is suppressed if the mixing with $q\overline{q}$ states is small.

In the search for resonances one usually looks first for peaks in the mass spectrum. If several states are overlapping, or in the presence of coherent "background", the peak position may be shifted or the resonance may even appear as a dip in the mass spectrum. The crucial characteristics of a resonance is therefore the energy dependence of the corresponding complex partial wave amplitude which moves along a full loop inside the "Argand diagram": besides the mass peak the phase variation has to be demonstrated.

Such results are obtained from energy independent phase shift analyses which try to determine the individual partial waves for a sequence of energy values. Usually such analyses are plagued by ambiguities. To start with, one can obtain a description of the scattering data in an energy dependent fit from an ansatz with a superposition of resonances. Such global fits to the mass spectra of mesonic systems in a broad range up to about 1700 MeV and including an increasing number of different reactions in (38) have been performed by several groups, starting with the CERN-Munich Collaboration [39,40], then by Au, Morgan and Pennington (AMP) [41,42], Lindenbaum und Longacre (LL) [43] and more recently by Bugg, Sarantsev and Zou (BSZ) [44] and by Anisovich, Prokoshkin and Sarantsev (APS) [16].

A survey of results from these representative global fits are given in Table 4. All these fits include the narrow $f_0(980)$, probably the only uncontroversial and well located f_0 state. Furthermore, they all show one rather broad state of more than 500 MeV width, called now $f_0(400-1200)$ by the PDG [18]; this state is considered as resonance $f_0(1000)$ in [42], otherwise it is just refered to as "background". In addition, states of higher mass are required by the fits but with masses which fluctuate from one fit to another. The PDG in their recent summary table includes the $f_0(1370)$ and the $f_0(1500)$ which also represents the states quoted earlier, the $f_0(1300)$ and $f_0(1590)$.

In Fig. 3 we show some recent results on the mass dependence of the isoscalar (I=0) S-wave $\pi\pi$ cross section as obtained by BNL-E852 [45] and GAMS Collaborations [16]. This mass spectrum with three peaks (the "red dragon") will be interpreted by us as a very broad state centered around 1 GeV (glueball) which interferes with the resonances $f_0(980)$ and $f_0(1500)$ whereby the dips near the respective resonance positions are generated.

In the following we will reexamine the evidence for resonances claimed in the different mass intervals, especially in the peak regions in Fig. 3 by studying the phase shift analyses in different processes and in particular the phase variation near the respective resonance masses.

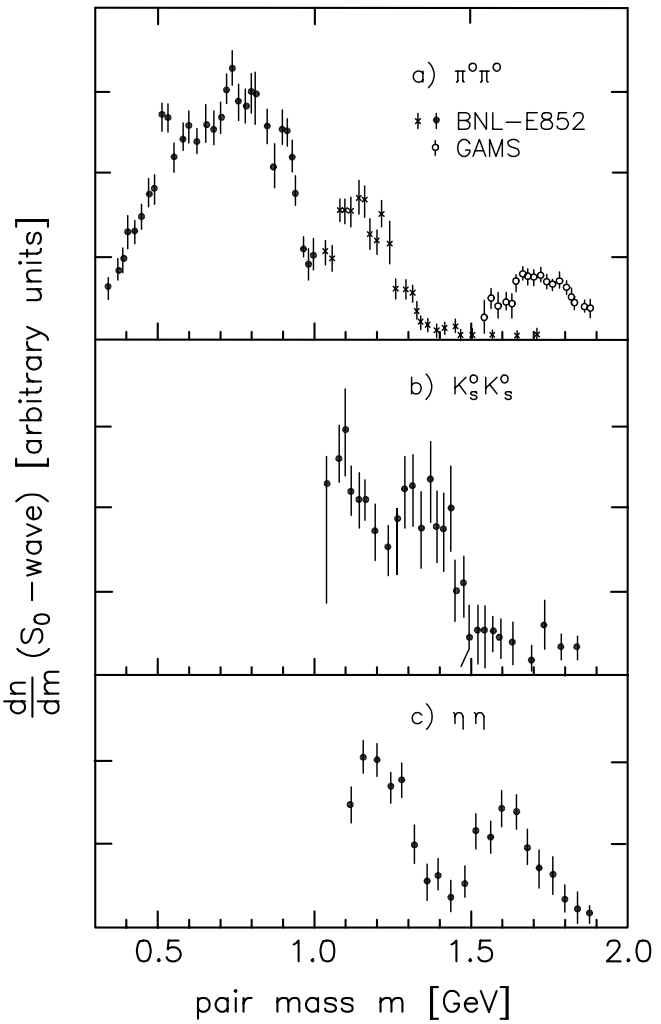

Fig. 3. Isoscalar S-wave components of the mass spectra of pseudoscalar pairs produced in πp-collisions at small momentum transfers t, (a) $\pi^0\pi^0$ spectrum, the prefered solution for $m < 1.5$ GeV by the BNL-E852 experiment [45] (preliminary results) and an alternative solution for higher masses by GAMS [16]; (b) $K_s^0K_s^0$ spectrum by Etkin et al. [84] which is similar to the results by Cohen et al. [82] below 1600 MeV and (c) $\eta\eta$ spectrum by Binon et al. [86]

3.1 The low energy $\pi\pi$ interaction ($m_{\pi\pi} \lesssim 1000$ MeV) and the claim for a narrow $\sigma(770)$ resonance

At low energies only the $\pi\pi$ channel is open. According to the common view which emerged in the mid of the 70's the isoscalar S-wave has negligable coupling to inelastic channels below the $K\overline{K}$ threshold and the phase shift δ_ℓ^I with $\ell = 0,\ I = 0$ moves much more slowly through the ρ meson region than the P-wave. This strong $\pi\pi$ interaction is interpreted either as "background" or as a very broad state as discussed above. Only near the $K\overline{K}$ threshold the phase varies rapidly because of the presence of the $f_0(980)$ resonance. There is an old claim for the existence of a narrow resonance $\sigma(770)$ under the ρ meson which

Table 4. Isoscalar states included in various global energy dependent fits to reactions (38) with channels a-d. For the broad state the poles of the scattering amplitude at $m - i\,\Gamma/2$ is given. Only one of the two states near the $f_0(980)$ found by AMP are kept in [42]

authors	broad state	other states	reactions
CM [39]	1049 - i 250 MeV	$f_0(980)$, $f_0(1537)$	1a
AMP [41]	910 - i 350 MeV	$f_0(988)$, $[f_0(991)]$, $f_0(1430)$	1a, 2, 5 7a,b 8, 9
LL [43]	1300 - i 400	$f_0(980)$, $f_0(1400)$, $f_0(1720)$	1, 2, 3, 6
BSZ [44]	A: 571 - i 420 MeV B: 1270 - i 530 MeV	$f_0(980)$, $f_0(1370)$, $f_0(1500)$	1, 2, 4
APS [16]	1530 - i 560 MeV	$f_0(980)$, $f_0(1370)$, $f_0(1500)$, $f_0(1780)$	1, 2, 3, 4

has been put forward again more recently arguing with results from polarized target.

Most results on the $\pi\pi$ S-wave obtained more than 20 years ago have been derived from the reactions

$$\text{(a)} \quad \pi N \to \pi\pi N \qquad \text{(b)} \quad \pi N \to \pi\pi \Delta \qquad (39)$$

in the $\pi^+\pi^-$ charge mode with unpolarized target in application of variants of the one-pion exchange (OPE) model (for a general review, see [46], for the low energy $\pi\pi$ interactions, see [47], for example). In this charge mode there is a twofold ambiguity ("up-down") for each energy interval which corresponds to either a narrow or a very broad resonance under the ρ meson. From the study of the $\pi^+\pi^-$ [48, 39, 40] and $\pi^0\pi^0$ data [49] the narrow resonance solution has finally been excluded [48, 50, 39, 40, 42].

The measurement of reaction (39a) with polarized target by the CERN-Cracow-Munich Collaboration [51, 52] has made possible a more detailed investigation of the production mechanisms but the analysis also leads to a new class of ambiguities in phase shift analysis.

In a recent reanalysis of these data Svec [53] finds in the modulus of one of the transversity amplitudes a narrow peak near 750 MeV, whereas in case of the other one a broad mass spectrum is observed. In Breit-Wigner fits to these mass spectra an extra state $\sigma(750)$ of width $\Gamma = 150$ MeV – or in the preferred fits even two σ states – are included besides the $f_0(980)$ resonance. In these considerations no attempt has been made to fit the amplitude phases nor to respect the partial wave unitarity which is important in particular near the inelastic threshold.

These constraints are taken into account in the subsequent analysis of the polarized target data by Kamiński, Leśniac and Rybicki (KLR) [54]. In the region below 1000 MeV they found four different solutions duplicating the old up-down ambiguity:

$$\begin{array}{ll} \text{(a) up-steep} & \text{(b) up-flat} \\ \text{(c) down-steep} & \text{(d) down-flat.} \end{array} \qquad (40)$$

Furthermore, a separation into pseudoscalar (π) and pseudovector (a_1) exchange amplitudes has been carried out.

The solution (40c) is excluded immediately as it leads to a strong violation of partial wave unitarity. The solution (40d) is essentially consistent with the previous result from the unpolarised target data [39] up to $m_{\pi\pi} \sim 1400$ MeV and the phase shift deviates by not more than 30° in the region above this mass.

The solution (40a) which is consistent with a narrow $\sigma(750)$ as in [53] also shows a systematic violation of unitarity and is therefore considered as "somewhat queer" by KLR but not excluded. However, both up solutions suffer from similar problems already discussed in connection with the old analyses:

(a) Comparison with the $\pi^0\pi^0$ final state

In this case the P-wave is forbidden and therefore the up-down ambiguity does not show up. The recent very precise data on the reactions 4 in (38) by the Crystal Barrel Collaboration [6, 11] can be interpreted in terms of $\pi\pi$ amplitudes using an isobar model for the annihilation process. The striking effects from the $f_0(980)$ state are clearly visible but the mass spectra around 750 MeV are rather structureless and there is no sign of a narrow resonance. In particular, the existence of a resonance with width around 250 MeV has been excluded in [11].

(b) Rapid variation of phase near $K\overline{K}$ threshold

The GAMS-Collaboration [55] has presented results on the S-wave magnitude of reaction 1b in (38) obtained from process (39a). Their results show a sudden decrease of the S-wave magnitude above a mass of 850 MeV with a narrow dip at 970 MeV. A dip of comparable type is also obtained for the KLR down-solution (Fig. 2a of [54]); the position of the dip is slightly moved upwards, presumably because of different isospin I=2 contributions. On the other hand, the up-solution reaches the minimum cross section already at the lower mass around 900 MeV in qualitative difference to the GAMS data. The GAMS collaboration so far has not yet published the original experimental results in terms of spherical harmonic moments. Once available the 4 different solutions from the polarized target experiment could be compared directly to the moments from the $\pi^0\pi^0$ final state which should determine the unique solution. The GAMS data are consistent again with fits

which properly take into account unitarity at the threshold such as in [44,16]. A similar behaviour in the mass region below ~ 1000 MeV is shown by the BNL-E852 data [45] (see also Fig. 3). These arguments favor the down-flat-solution which agrees with the results obtained previously. All other choices would lead to serious inconsistencies with general principles or with other experimental results. Nevertheless, it would be desirable to obtain the complete results and a common description of the reactions (39) in the $\pi^+\pi^-$ and $\pi^0\pi^0$ charge modes.

3.2 How reliable are $\pi\pi$ scattering results from unpolarised target experiments?

It may be surprising at first sight that the results from polarized and unpolarized target are so similar, as found by KLR [54]. In fact, it is occasionally claimed (especially in [53]) that the analyses from unpolarized target experiments are obsolete because of the importance of a_1-exchange besides π-exchange. Most results obtained so far on elastic and inelastic $\pi\pi$ interactions 1-3 in (38), which are important in the subsequent discussion, have been obtained from unpolarized target experiments. Therefore, it is appropriate at this point to contemplate the consequences to be drawn from the experiments with polarized target.

Motivated by the OPE model with absorptive corrections, the commonly applied procedure to extract the production amplitudes from the unpolarized target experiment, has been based on the following two assumptions [56–58] concerning the nucleon helicity flip and non-flip amplitudes $f^{\pm}_{\ell,\mu}$ and $n^{\pm}_{\ell,\mu}$ with natural (+) and unnatural (−) parity exchange for production of a mesonic system with spin ℓ and helicity μ:

(i) Spin-flip dominance: the non-flip amplitudes $n^{\pm}_{\ell,\mu}$ vanish, at least the (−) amplitudes, which are *not* generated by absorbed OPE at high energies (this allows for $a_2(2^{++})$-exchange but not for $a_1(1^{++})$-exchange).
(ii) Phase coherence: The phases of the production amplitudes at fixed mass $m_{\pi\pi}$ and momentum transfer t between the incoming and outgoing nucleons depend only on $\pi\pi$ spin ℓ and not on the helicities.

A further simplification can be obtained if t-integrated moments are used in the "t-channel frame" [59]. These assumptions yield an overdetermined system of equations. It can be solved for the amplitudes up to some discrete ambiguities whereby the constraints are found to be well satisfied [39]; results from "Chew-Low extrapolation" in t and from t averaged moments yield comparable results [60].

The polarized target experiment has clearly demonstrated the existence of the a_1 exchange process [51,52] which contributes to the non-flip amplitudes invalidating assumption (i). However, for the amplitude analyses carried out in an unpolarized target experiment – such as in [39,60] – weaker assumptions than the ones above are sufficient to obtain the same results [56], namely

(i′) nucleon helicity flip and non flip amplitudes f and n are proportional

$$n^{+}_{\ell,\mu} = \alpha^{(+)} f^{+}_{\ell,\mu}, \qquad n^{-}_{\ell,\mu} = \alpha^{(-)} f^{-}_{\ell,\mu} \tag{41}$$

for natural (+) and unnatural (−) exchange separately for any dipion spin and helicity ℓ, μ.
(ii′) as in (ii) but there may be an overall phase difference between (+) and (−) amplitudes.

Then also the transversity up and down amplitudes g and h which are determined in the polarized target experiment

$$g^{\pm}_{\ell,\mu} = \frac{1}{\sqrt{2}}(n^{\pm}_{\ell,\mu} \mp f^{\pm}_{\ell,\mu}), \qquad h^{\pm}_{\ell,\mu} = \frac{1}{\sqrt{2}}(n^{\pm}_{\ell,\mu} \pm f^{\pm}_{\ell,\mu}) \tag{42}$$

should be proportional

$$\frac{|g^{\pm}_{\ell,\mu}|}{|h^{\pm}_{\ell,\mu}|} = \frac{|\alpha + i|}{|\alpha - i|}. \tag{43}$$

This relation is approximately fulfilled and the ratio is found $\frac{|g|}{|h|} \approx 0.6$ for S,P,D and F waves over the full mass range explored in the small $|t| < 0.15$ GeV region (Fig. 6 in [52]); however, the fluctuation of the data is quite large and local deviations cannot be excluded. In a restricted analysis using only S and P waves below 900 MeV some trend of this amplitude ratio with mass was found [51] but the D-waves can certainly not be neglected here.

It is pointed out by KLR [54] that in the narrow regions where the S-wave magnitude is small, i.e. around 1000 MeV and 1500 MeV the a_1 contribution may become as large as the π exchange contribution, whereas otherwise it amounts to only about 20% of it.

With one pion exchange only (modified by absorption) the ratio (43) would have to be unity, so the modification (41) amounts only to a change of the overall adjustment of normalization in the energy dependent fits.

It is very satisfactory that the down-solution for the S-wave which we preferred above is also consistent with the energy independence of the amplitude ratio $\frac{|g|}{|h|} \approx 0.6$ (Fig. 2b in [54]) whereas the disfavored up solution with the narrow σ would lead to an increase of this ratio by up to a factor of 2 just in the mass interval of ambiguity 800-1000 MeV. Such exceptional behaviour of amplitudes is not plausible.

As to the simplifying assumption (ii) on the phase coherence of amplitudes the data from polarized target are confirming it in their general trend but there are overall shifts of amplitude phases of up to about 20°, only some relative phases involving the D-wave amplitudes indicate larger differences (Figs. 8,9,10 in ([52])).

In summary, the original assumption (i) has been demonstrated by the polarized target experiment to be clearly violated; the modified assumption (i′) is still approximately correct within the given accuracy, whereas some moderate violations of phase coherence (ii′) have been seen. This explains why the phase shift results from the polarized target experiment – looking at the preferred

solution – are not very different from the previous findings, in particular, there is no evidence for entirely new states, such as a $\sigma(750)$.

The proportionality (41) is expected, in particular, if the amplitudes $a_1\pi \to \pi\pi$ and $\pi\pi \to \pi\pi$ are proportional and appear as factors in the production amplitudes. In general, such a relation may be violated as different resonant states could have different couplings to the $\pi\pi$ and $a_1\pi$ channels, also there could be different signs. However, as long as the a_1 exchange is small, such as in the small t region, the violation of the assumption can play only a role at this reduced level. On the other hand, one has to be careful in applications of the above assumptions in kinematic regions where OPE is not dominant (for example, large t).

3.3 Interference of the $f_0(980)$ with the "background" and the molecule hypothesis

In elastic $\pi\pi$ scattering the narrow $f_0(980)$ interferes with the large "background", now also called $f_0(400-1200)$ and appears as a dip in the S-wave cross section [48,39]. There are other processes where to the contrary the $f_0(980)$ appears as a peak. This phenomenon has been observed first in pion pair production with large momentum transfer $|t| \gtrsim 0.3$ GeV [61] and more recently by GAMS [55]. Fits to the peak yield values for the total width of $\Gamma = 48 \pm 10$ MeV. A direct clear evidence for the phase variation according to a Breit-Wigner resonance can be inferred from the interference pattern of the rapidly varying resonance amplitude with the tail of the $f_2(1270)$ in reaction (3a) at large t as measured by the GAMS Collaboration [55].

The interference of this narrow resonance with the background varies from one reaction to the other. In this way one can see that this "background" has its own identity. The reactions in (38) with a $\pi\pi$ system in the final state can be classified roughly into 3 groups according to the different appearence of the $f_0(980)$ in the mass spectrum:

(a) dip in reaction 1, indication of dip in reaction 4a [6, 62];
(b) peak in reaction 1 in large t production, and in 5a [63–65], 5c [66], 9a [67–69];
(c) an interference of the $f_0(980)$ Breit-Wigner amplitude with a background amplitude of positive real part is suggested in 4b [7] and in a similar way in 7 [71,70].

The different interference patterns are naturally attributed to the different couplings of the $f_0(980)$ and of the "background" to the initial channel.

The dip is observed in the elastic $\pi\pi$ channel. In this case the background amplitude is near the unitarity limit and the additional resonance has to interfere destructively. The reaction 4a shows a small dip around 950 MeV followed by a peak near 1000 MeV and fits into group (a) or (b). All other processes are inelastic.

In particular, the transmutation of a dip into a peak in $\pi N \to \pi\pi N$ with increasing momentum transfer can be explained by the assumption of an increasing importance of a_1 exchange over π exchange with

$$|A(\pi a_1 \to f_0(980) \to \pi\pi)| \gg |A(\pi a_1 \to f_0(400-1200) \to \pi\pi)|. \quad (44)$$

In this case the peak occurs, either because the background interferes constructively, or because it becomes too small.

There is some support for this interpretation from the KLR results [54] discussed above on the polarized target data at small $|t| < 0.2$ GeV. For the favored "down-flat" S-wave solution the modulus of the a_1-exchange amplitude shows a peak (significance about 2σ) just in the mass interval 980-1000 MeV whereas the pion exchange amplitude shows a dip in the region 980-1060 MeV (see Fig. 7a in [54]).

Similar conclusions concerning different exchange mechanism has been drawn in the recent paper by Achasov and Shestakov [72] where detailed fits including a_1-exchange are presented.

A remarkable similarity is seen in the interference pattern of the two reactions in group (c) where a small peak near 950 MeV is followed by a large drop near 1000 MeV. In reaction 4b the initial $p\overline{p}$ state must be in a η, η' type state, so the $\pi\pi$ state couples to two isoscalars, similarly in reaction 7 if the initial state is formed by two isoscalar pomerons. This is in marked difference to the pattern seen in $p\overline{p} \to 3\pi^0$ where four isovectors couple together. This shows that the $f_0(980)$ and the "background" must have different flavor composition although they have the same quantum numbers.

Finally, we comment on the hypothesis [30], $f_0(980)$ could correspond to a $K\overline{K}$ molecule (or other 4q system), which is adopted in various contemporary classification schemes (see Sect. 2). S-matrix parametrizations have been used to argue both ways, against [42] or in favor [73] of such a hypothesis. If the $a_0(980)$ and $f_0(980)$ are such bound states one has to worry that the successful quark model spectroscopy is not overwhelmed by a large variety of additional hadronic bound states. On the phenomenological side, if the $f_0(980)$ is a loosely bound system, then, in a violent collision with large momentum transfer one would expect an increased probability for a break-up. The GAMS data, however, demonstrate the opposite, the persistence of $f_0(980)$ with respect to the background. Furthermore, a recent investigation by the OPAL Collaboration [74] has shown the production properties of the $f_0(980)$ to be very similar to those of the $q\overline{q}$ states $f_2(1270)$ and $\phi(1020)$ nearby in mass in a variety of measurements. Therefore, we do not feel motivated to give up $f_0(980)$ as genuine $q\overline{q}$ state but we suggest a flavor composition different from the one of the "background".

3.4 The mass region between 1000 and 1600 MeV

This includes the mass range from the $f_0(980)$ up to the $f_0(1500)$. Near both resonance positions there are dips in the elastic $\pi\pi$ S-wave cross section (see Fig. 3). For this region the PDG lists – besides the $f_0(400-1200)$ – the

$f_0(1370)$ state; there may actually be two states, one seen as a large effect in the elastic $\pi\pi$ scattering, the other one being strongly inelastic. We will reconsider now the evidence from phase shift analyses for states in this mass interval.

3.4.1 Elastic and charge exchange $\pi\pi$ interaction

Phase shift analyses have been performed using the CM data from unpolarized target [39,75,60] and by the Omega spectrometer group [76]. One finds here a number of ambiguous solutions which are discussed in terms of Barrelet zeros [77]. Namely, for a finite number of partial waves the amplitude can be written as a polynomial in $z = \cos\vartheta$. Then the measurement of the cross section differential in the scattering angle ϑ determines the real parts and the moduli of the imaginary parts of the amplitude zeros z_i. The different solutions can then be classified according to the signs of $\mathrm{Im}z_i$.

In [75] four solutions for elasticities η_ℓ^I and phase shifts δ_ℓ^I are presented distinguishing the signs of Im z_i at 1500 MeV for $i = 1,2,3$ as $(---)$, $(-+-)$, $(+--)$ and $(++-)$ and assuming a sign change of $\mathrm{Im}z_1$ at 1100 MeV. They correspond to the solutions A, C, $\overline{\mathrm{B}}$ and $\overline{\mathrm{D}}$ in [60]. Yet more solutions are given in [60,76] corresponding to different branches near 1100, 1500 and above 1800 MeV. The comparison with $\pi^0\pi^0$ data [78,76] left the solutions C and D as unfavored. Solution A is also consistent with the energy dependent result of CM [39] up to 1500 MeV where $\delta_0^0 \approx 156^o$, whereas solution $\overline{\mathrm{B}}$ reaches $\delta_0^0 \approx 165^o$. Some descendents α, β and β' are obtained from solutions A and B if constraints from dispersion relations are taken into account [79].

The data from polarized target [52,54] essentially lead to a unique solution in this mass range as the imaginary parts of zeros came out rather small

$$\begin{aligned} \text{Im } z_1 &\sim 0 \quad \text{for} \quad m_{\pi\pi} > 1100 \text{ MeV} \\ \text{Im } z_2 &\sim 0 \quad \text{for} \quad m_{\pi\pi} > 1400 \text{ MeV} \end{aligned} \tag{45}$$

so that the various solutions are not significantly different any more. The results for the phase shifts δ_0^0 in [54] are again similar to solution A in [60] or to the energy dependent phase shift solutions in CM [39] up to $m_{\pi\pi} \sim 1400$ MeV; some additional variation is indicated above this energy in both δ_0^0 and η_0^0.

Furthermore we note two aspects of the polarized target results

(a) The S-wave is near the unitarity limit in $1150 \lesssim m_{\pi\pi} \lesssim 1450$ MeV and drops to zero at $m_{\pi\pi} \sim 1500$ MeV (Fig. 2 in [52]).
(b) The phase difference of S and D wave amplitudes changes sign in both g and h transversity amplitudes with

$$\begin{aligned} \varphi_S - \varphi_D &> 0 \quad \text{for} \quad m_{\pi\pi} < 1250 \text{ MeV}, \\ \varphi_S - \varphi_D &< 0 \quad \text{for} \quad m_{\pi\pi} > 1350 \text{ MeV}. \end{aligned} \tag{46}$$

The phase differences (Fig. 9,10 in [52]) are best met by the previous solution β', the result (b) excludes solution B. The drop of intensity (a) is not so well reproduced by the previous phase shift analyses of unpolarized target experiments.

Next we turn to the charge exchange reaction $\pi^+\pi^- \to \pi^0\pi^0$ which should help to select the unique solution for the S-wave. There are three relevant experiments: (a) IHEP-NICE [80], (b) GAMS [55] and (c) BNL – E852 (preliminary results [45]).

In (a) the amplitude S_0 is obtained after subtraction of the I=2 contribution. One finds two different solutions for S_0, one inside the unitarity circle with $0.5 \lesssim \eta_0^0 \lesssim 1$, and another one with larger modulus which exceeds by far the unitarity limit. The physical solution has

$$\varphi_S - \varphi_D < 0 \quad \text{for} \quad m_{\pi\pi} > 1100 \text{ MeV}. \tag{47}$$

The two solutions branch around $m_{\pi\pi} = 1100$ MeV where $\cos(\varphi_S - \varphi_D) \approx 1$. The sign change is similar to the result (46) above in the charged $\pi\pi$ mode.

The first results from (c) at small momentum transfer t with higher statistics give a similar picture: The amplitude with the smaller modulus is the physical solution. The modulus shows again a sharp drop at 1000 and 1500 MeV. There is a strong inelasticity immediately above 1000 MeV and a small phase shift rise by about 30^o if $m_{\pi\pi}$ increases from 1000 to 1300 MeV, in qualitative agreement with the CM result [39].

In the GAMS experiment (b) with high statistics one finds again the two solutions with large and small amplitude modulus peaking at $m_{\pi\pi} \sim 1200$ MeV and the dips at 1000 and 1500 MeV. There is no attempt, however, to determine the phase shifts and to consider the role of unitarity. In fact, the solution with large modulus is declared as the physical one. The phase difference $\varphi_S - \varphi_D$ stays positive in the full mass range: it is falling for $m_{\pi\pi} < 1100$ MeV as in (46) but it is rising again in the range from 1100 to 1400 MeV – contrary to all solutions A-D in [60] and the one in [52]. Such behaviour would imply the S wave phase φ_S to rise more rapidly than the resonant D wave phase φ_D which is highly unplausible. Possibly a transition from one solution to the other one around $m_{\pi\pi} \sim 1200$ MeV – consistent with (46) – is allowed within the errors which would resolve this conflict.[3] One should also consider the possibility of small phase shift differences due to a_1 exchange as suggested by the polarized target experiment and discussed in Sect. 3.2. Such systematic effects could be studied further from the angular distribution moments which have not been presented so far.

In summary, the various phase shift analyses of $\pi\pi$ scattering suggest the isoscalar S wave under the $f_2(1270)$ to be slowly moving with an inelasticity between 0.5 and 1. This does not correspond to a resonance of usual width. We can estimate the width Γ of a hypothetical resonance near $m_{\pi\pi} \sim 1300$ MeV from the energy slope of the phase

[3] Taking the data on $|S|^2$, $|D|^2$ and $|S||D|\cos(\varphi_S - \varphi_D)$ presented in [81] at face value we obtain unphysical values $\cos(\varphi_S - \varphi_D) > 1$ at $m_{\pi\pi} \sim 1200$ MeV.

shifts δ_0^0. Using the data from CM [39] or KLR [54] we find

$$\frac{d\delta_0^0}{dm_{\pi\pi}} = \frac{2}{\Gamma}\frac{1+\eta_0^0}{2\eta_0^0} \approx 3.7 \text{ GeV}^{-1} \tag{48}$$

in the mass range $1100 \lesssim m_{\pi\pi} \lesssim 1400$ MeV which yields a lower limit on the width

$$\Gamma[f_0(1300)] \ > \ 540 \text{ MeV}. \tag{49}$$

where the inequality corresponds to $\eta_0^0 < 1$. This estimate shows that the slow movement of the phase does not allow the interpretation in terms of a usual narrow resonance. On the other hand, there is evidence for a rapid drop in the S-wave intensity near 1500 MeV indicating a Breit-Wigner type narrow resonance around this mass. An analysis which would treat both the elastic and charge exchange $\pi\pi$ scattering data together in this mass range has not yet been carried out but is highly desirable.

3.4.2 The reaction $\pi\pi \to K\overline{K}$

It is argued by BSZ [44] that the influence of the additional scalar state $f_0(1370)$ is marginal for the $\pi^+\pi^-$ (CM) data whereas it becomes essential in the $K\overline{K}$ final states. The study of this final state is more difficult than $\pi\pi$ as resonances with both G parities can occur in a production experiment where besides one pion exchange also exchanges with $G = +1$ particles may contribute.

Phase shift analyses of the $K\overline{K}$ system have been carried out (a) at Argonne [82], (b) by the Omega spectrometer experiment at CERN [83] and (c) at BNL [84]; (d) the moduli of the partial wave amplitudes in the K^+K^- final state have been obtained also from a CERN-Krakow-Munich experiment with polarized target [85].

In the Argonne experiment (a) a comprehensive analysis of three reactions

$$\pi N \to K\overline{K}N' \tag{50}$$

in different charge states has allowed the separation of partial waves in both isospin states I=0 and I=1. In the mass region below 1500 MeV S, P and D waves have been included and 8 different partial wave solutions have been obtained in the beginning. Requirements of charge symmety, reasonable t-dependence for the pion exchange reactions and approximate behaviour of the P waves as tails of the ρ and ω resonances have finally selected a unique solution (called Ib). The absolute phase of the amplitude is determined relative to the Breit-Wigner phase of the D wave resonances $f_2(1270)$ and $a_2(1320)$. It is remarkable that the P waves of the preferred solution are compatible both in magnitude and phase with what is expected for the tails of the vector mesons.

The preferred solution shows two features

(i) The modulus of the S_0 amplitude has a narrow peak near threshold – possibly caused by the $f_0(980)$ – and shows an enhancement near 1300 MeV before it drops to a small value near $m_{K\overline{K}} \sim 1600$ MeV (see Fig. 3b).

(ii) The phase stays nearly constant up to $m_{K\overline{K}} \sim 1300$ MeV, thereafter it advances by $\Delta\delta_0^0 \sim 100^o$ when approaching $m_{K\overline{K}} \sim 1500$ MeV and then drops.

This phase variation is similar to the one in elastic $\pi\pi$ scattering ($\Delta\delta_0^0 \sim 100^o$ in KLR [54] and $\Delta\delta_0^0 \sim 70^o$ in CM [39]) and lead to the conclusion [82] that the phase variation in $K\overline{K} \to K\overline{K}$ is small and that the phase variation in $\pi\pi \ \to \ K\overline{K}$ is related to a resonance $\epsilon(1425)$ which couples mainly to $\pi\pi$.

The other two experiments (b) and (c) extend their analysis towards higher masses which leads to more ambiguities. In the mass region considered here below 1600 MeV there is close similarity with the Argonne results in the two features (i) and (ii) above: in (b) one of the two ambiguous solution agrees whereas the second corresponds to a narrow resonance in the S-wave with $m_{\pi\pi} = 1270$ MeV and $\Gamma = 120$ MeV whereas in (c) the favored solution agrees except for an additional phase variation below 1200 MeV by 30^o. In addition the continuation to higher masses with a suggested resonance at 1770 MeV is presented. In the region below 1200 MeV ($\cos(\phi_S - \phi_D) \approx -1$ at 1200 MeV) another solution should be possible with $\phi_S - \phi_D \ \to \ \pi - (\phi_S - \phi_D)$; this choice would yield a slightly decreasing phase ϕ_S similar to the one in (a); the D-wave phase ϕ_D presented in (c) in this region is decreasing which would contradict the expected threshold behaviour. In (a) the phase near threshold has been fixed by comparison with the P-wave taken as tail of the ρ meson. All these experiments are consistent with a solution with slow phase variation around 1300 MeV.

Only experiment (d) shows a different result which resembles the alternative solution in (b) without peak in the S-wave near 1300 MeV emphasized in (i) and has been rejected in [82] and also in [84] where no ambiguity exists contrary to the K^+K^- channel. No discussion of ambiguities in terms of Barrelet zeros nor results of a phase shift analysis has been presented. For the moment we assume that the analysis in (d) did not find all ambiguous solutions and so does not invalidate the preferred solution quoted above.

We summarize the results from experiments (a)-(c) on the parameters of the resonance $\epsilon(1420)$ as obtained from the fits to the phases in Table 5. The comparison of the ϵ resonance parameters with the PDG numbers in the last line suggests the identification

$$\epsilon(1420) \to f_0(1500) \tag{51}$$

because of comparable width and small $K\overline{K}$ coupling although there is a small shift in mass; the latter is smallest in a energy dependent fit over the full mass range.

For further illustration we show in Fig. 4a the S-wave in an Argand diagram we obtained as smooth interpolation of the results by Etkin et al. [84]. After an initial decrease of the amplitude from its maximum near threshold a resonance circle develops in the region 1200-1600 MeV with small phase velocity at the edges and largest velocity in the interval 1400-1500 MeV suggesting a resonance pole with negative residue. The small dip at 1200 MeV appears, as the resonant amplitude moves first in negative

Table 5. Different determinations of resonance parameters in $K\overline{K}$ final state near 1500 MeV

group	mass range of fit [MeV]	mass [MeV]	width [MeV]	$\Gamma_{K\overline{K}}/\Gamma_{\pi\pi}$
Argonne [82]	1000 - 1500	1425 ± 15	160 ± 30	0.1 - 0.2
OMEGA [83]	<1550	∼ 1400	∼ 170	
BNL [84]	1000 - 2000	1463 ± 9	118^{+138}_{-16}	
PDG [18]: $f_0(1500)$		1500 ± 10	112 ± 10	0.19 ± 0.07

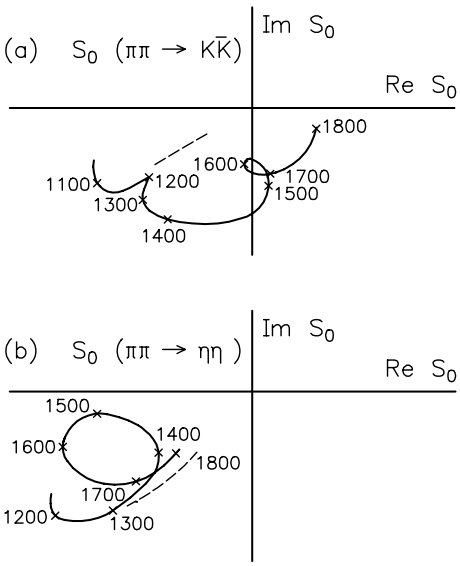

Fig. 4. Argand diagrams of the isoscalar S-wave amplitudes representing the data on the mass spectra shown in Fig. 3 and the relative phases between S and D-waves assuming a Breit-Wigner form for the latter (data from [84] and [86]). The numbers indicate the pair masses in MeV, the dashed curve represents an estimate of the background

direction of ReS_0 (to the "left") above the background which moves slowly to the "right". This interference phenomenon yields the peak near 1300 MeV in Fig. 3b, but there is no evidence for an extra loop corresponding to the additional state $f_0(1370)$. The Argand diagram presented by Cohen et al. [82] for masses below 1600 MeV shows a qualitatively similar behaviour.

3.4.3 The reactions $\pi\pi \to \eta\eta,\ \eta\eta'$

These reactions have been studied by the IHEP-IISN-LAPP Collaboration [86,87] again in πp collisions applying the OPE model with absorptive corrections. The partial wave decomposition of the $\eta\eta$ channel yields an S wave with an enhancement which peaks near 1200 MeV and a second peak with parameters

$$m_G = (1592 \pm 25)\ \text{MeV}, \qquad \Gamma_G = (210 \pm 40)\ \text{MeV}. \tag{52}$$

This state G(1590) has been considered as a glueball candidate by the authors as in this mass range there are no resonance signals from $K\overline{K}$ nor from $\pi^0\pi^0$. The phase difference $\varphi_D - \varphi_S$ varies with mass in a similar way as the one in the $K\overline{K}$ final state: it rises from 210° at 1200 MeV up to the maximum of 300° at around 1500 MeV and then drops (see, for example [84]). Therefore a similar interpretation is suggested. The $f_2(1270)$ interferes with the S-wave which is composed of one Breit-Wigner resonance around 1500 - 1600 MeV above a background with slowly varying phase.

There is nevertheless a major difference between both channels if the S-wave magnitude is considered. At its peak value in $\eta\eta$ near 1600 MeV there is a minimum in $K\overline{K}$ and the opposite behaviour around 1300 - 1400 MeV, namely a peak in $K\overline{K}$ and a dip in $\eta\eta$ (see Fig. 3b,c). Both phenomena can be explained by a change in the relative sign between the background and the resonance amplitude.

In Fig. 4b we show the behaviour of the S-wave amplitude which we obtained using the data by Binon et al. [86]. Assuming a Breit-Wigner phase for the $f_2(1270)$ one finds that the S-wave phase around 1300 MeV is slowly varying again. At higher energies a contribution of about 20% from $f_2(1520)$ is expected in the D-wave as in the $\pi\pi \to K\overline{K}$ channel. Now the resonance circle in Fig. 4b corresponds to a pole in the amplitude with positive residue and this explains the rather different mass spectra emphasized above in the $K\overline{K}$ and $\eta\eta$ channels.

The situation may be illustrated by the following simple model for the S and D-wave amplitudes

$$\begin{aligned} &\pi\pi \to K\overline{K}: S = B_K(m) - x_K^{(0)} f_0(m) e^{i\phi_K};\ D = x_K^{(2)} f_2(m) \\ &\pi\pi \to \eta\eta: \quad S = B_\eta(m) + x_\eta^{(0)} f_0(m) e^{i\phi_\eta};\ \ D = x_\eta^{(2)} f_2(m) \end{aligned} \tag{53}$$

where $B_i(m)$ denotes the slowly varying background amplitudes with Re$B_i < 0$ and $f_\ell(m)$ the Breit-Wigner amplitudes for spin ℓ with $f_\ell(m_{res}) = i$ and elasticities $x_i^{(\ell)}$; ϕ_i is an additional small phase due to background.

Then, despite the rather large mass difference between $\epsilon(1420)$ and $G(1590)$ of 170 MeV, we can consider both states as representing the same resonance interfering with the broad background and therefore suggest

$$G(1590) \to f_0(1500). \tag{54}$$

The $\eta\eta$ experiment has been repeated at higher beam energy which allows the study of higher mass states. In the lower mass region the previous results are essentially recovered [88].

The $\eta\eta'$ mass spectrum [87] shows a threshold enhancement around 1650 MeV which the authors interpret as another signal from G(1590).

3.4.4 $p\overline{p}$ annihilation and the $f_0(1370)$ and $f_0(1500)$ states

The Crystal Barrel (CB) Collaboration at the LEAR facility at CERN has measured the $p\overline{p}$ annihilation reaction at rest. In this case the initial $p\overline{p}$ system is in either one of the three J^{PC} states

$$\begin{aligned} &{}^1S_0\ (0^{-+}), \quad {}^3P_1\ (1^{++}), \quad {}^3P_2\ (2^{++}) \quad \text{with} \\ &I^G\ =\ 1^- \text{ or } 0^+. \end{aligned} \tag{55}$$

Another experiment has been carried out at the Fermilab antiproton accumulator (E-760) at the *cms* energies $\sqrt{s}$ of 3.0 and 3.5 GeV. The following final states have been investigated (with I^G in brackets assuming isospin conservation)

$$\begin{aligned} &(a)\ \pi^0\pi^0\pi^0\ (1^-) \qquad (b)\ \pi^0\pi^0\eta\ (0^+) \qquad (c)\ \eta\eta\pi^0\ (1^-) \\ &(d)\ \eta\eta'\pi^0\ (1^-) \qquad (e)\ \eta\eta\eta\ (0^+) \end{aligned} \tag{56}$$

Reaction (a) has been studied by CB with the very high statistics of 712 000 events [6]. The Dalitz plot shows clearly the narrow band of low density (region A) corresponding to the $f_0(980)$ as also seen in the elastic $\pi\pi$ cross section. In the projection to the $\pi^0\pi^0$ mass the broad structureless bump peaking near 750 MeV and the sharper peak due to the $f_2(1270)$ are seen. The new feature is the peak at around 1500 MeV which corresponds to a band of about constant density in the Dalitz plot; therefore its quantum numbers are determined to be $J^{PC} = 0^{++}$ and the state is now called $f_0(1500)$. A peak of similar position and width is seen at the higher energies of E-760 [62] together with an increased $f_2(1270)$ signal and a decreased low mass bump. It is therefore likely that the same state $f_0(1500)$ is observed here although the authors consider it as a $f_2(1520)$ state. This conflict could be solved by means of a phase shift analysis. A weak signal of the same state is seen in reaction (b) at the higher energies.

The state $f_0(1500)$ is also identified by CB in reaction (c) where it appears as clear peak in the $\eta\eta$ mass spectrum and band in the Dalitz plot [8,89]. A significant signal is again seen at the higher $p\overline{p}$ energies [90]. Furthermore, Amsler et al. relate the threshold enhancement seen in the reaction (d) to the $f_0(1500)$ [9]. It is suggestive to identify this state with the resonance discussed before in this section where also the phase variation has been observed directly and to consider the $f_0(1500)$ as a genuine Breit-Wigner resonance.

In the region between the $f_0(980)$ and $f_0(1500)$ Amsler et al. claim the existence of a further scalar state, the $f_0(1370)$. In reaction (a) it is required by the fit as background under the $f_2(1270)$ very much as in $\pi\pi$ scattering. In reaction (c) it actually appears as clear bump with rather broad width of $\Gamma = 380$ MeV. On the other hand this bump has disappeared entirely at the higher *cms* energies [90], whereas the $f_0(1500)$ stays. This indicates a different intrinsic structure of both states; the disappearence of the $f_0(1370)$ at higher energies is reminiscent to the disappearence observed by GAMS of the peak at 700 MeV at production with large t in comparison with the $f_0(980)$ (see Sect. 3.3).

In the $p\overline{p}$ reaction a direct phase shift analysis as in the $\pi\pi$ scattering processes is not possible. The amplitudes for the different initial states (55) are constructed with the angular distributions specified in [91] and an ansatz for the $\pi\pi$ amplitudes within the framework of an isobar model. Unitarity constraints cannot be strictly enforced here as in case of two body $\pi\pi$ scattering processes. The evidence for the $f_0(1370)$ is based on the fits of this model to the Dalitz plot density.

In the fit by BSZ [44] the CB data have been described with inclusion of the $f_0(1370)$. Their fit predicts a rapid decrease of the phase in the channel $\pi\pi \to K\overline{K}$ near 1200 MeV; this variation is consistent with the BNL data [84] within their large errors but not with the slowly varying phases determined by Cohen et al. [82] with smaller errors. Furthermore a small dip is expected for the S-wave magnitude $|S|$ near the top which is neither observed in the GAMS [55] nor in the BNL [45] experiments on the $\pi^0\pi^0$ final state.

For the moment, we do not accept the $f_0(1370)$ effect as a genuine Breit-Wigner resonance. It appears to us that the Dalitz plot analysis of the $p\overline{p}$ data – although some phase sensitivity is given – is less selective than the phase shift analysis of two-body processes. The $\pi\pi$, $K\overline{K}$ and $\eta\eta$ data discussed in the previous subsections (Figs. 3,4) speak against a resonance interpretation of the peak at 1370 MeV.

4 The $J^{PC} = 0^{++}$ nonet of lowest mass

After the reexamination of the evidence for scalar states in the region up to about 1600 MeV we are left with the $f_0(980)$ and $f_0(1500)$ resonances where we have clear evidence for a peak and for the phase variation associated with a Breit-Wigner resonance. The identification of states in this mass region is so difficult because of their interference with the large background. As explained in the previous section, we do not consider the $f_0(1370)$ signal as evidence for a Breit-Wigner resonance in between the two f_0 states, but rather as the reflection of a yet broader object or the "background".

As members of the scalar nonet we consider then the two f_0 states besides the well known $a_0(980)$ and the

Table 6. Branching ratios $X_V^{(\pm)}$ for decays of J/ψ into vectormesons V and scalar (+) or pseudoscalar (−) particles according to the PDG [18]

decay modes	symbol	branching ratios $\times\ 10^4$
$J/\psi \to \varphi\ \eta\,'\,(958)$	$X_\varphi^{(-)}$	$3.3\ \pm\ 0.4$
$\varphi\ f_0\ (980)$	$X_\varphi^{(+)}$	$3.2\ \pm\ 0.9$
$\omega\ \eta\,'\,(958)$	$X_\omega^{(-)}$	$1.67\ \pm\ 0.25$
$\omega\ f_0\ (980)$	$X_\omega^{(+)}$	$1.41\ \pm\ 0.27\ \pm\ 0.47$

$K_0^*(1430)$. We will now have to clarify whether this assignment provides a consistent picture for the various observations at a given singlet-octet mixing angle to be determined. Such observations, together with further consequences of our hypotheses, will be discussed next.

4.1 Properties of $f_0(980)$ and $f_0(1500)$ from $J/\psi \to V\ f$ decays

There are three (primary) mechanisms – all without full analytic understanding – which contribute to purely hadronic decays of J/ψ into noncharmed final states:

1. $c\ \bar{c}$ annihilation into three gluons;
2. $c\ \bar{c}$ mixing with noncharmed virtual vector mesons $(\omega_V,\ \varphi_V,\ 3g_V)$,
   here $3g_V$ denotes a three gauge boson "state" with $J^{\,PC_n} = 1^{--}$;
3. $c\ \bar{c}$ annihilation into a virtual photon.

In each channel above the hadronization into a given exclusive, hadronic final state has to be included.

We will *assume* that the mechanism 1. above is the dominant one for the decay modes listed in Table 6. This Table involves only the pseudoscalar-scalar associated pair $(\eta\,'\,(958)\ ,\ f_0\ (980))$, i.e. only $f_0\ (980)$ from the scalar nonet, whereas no information is extracted at present for the associated decay modes into $\varphi\ f_0\ (1500)$ and $\omega\ f_0\ (1500)$ by the PDG [18].

A word of caution on the list in Table 6 is in order. The data for $\omega\ f_0\ (980)$ are based upon a single experiment (DM2 [66]) and therein essentially on a single data point. The result is supported however by the Mark II experiment [63] in which the recoil spectrum against the $f_0\ (980)$ is measured. The ratio of the ω and φ peaks are consistent with the ratio following from Table 6 although there is some uncertainty about the background under the φ meson.

With this remark in mind we have a closer look at Table 6. The entries for the decays into the scalar and pseudoscalar particles show an indicative *pattern* [4]:

$$X_V^{(+)} \approx X_V^{(-)} \to X_V \quad ; \qquad X_\varphi \approx 2\, X_\omega, \tag{57}$$

i.e. the branching fractions into the $\eta\,'\,(958)$ and the $f_0\ (980)$ are very similar which then suggests a similar quark composition.[5] We thus decompose both states $\eta\,'\,(958)$ and $f_0\ (980)$ according to their respective strange (s) and nonstrange (ns) $q\bar{q}$ composition, neglecting their small mass difference,

$$\begin{aligned} \eta\,'\,(958) &\sim c_{ns}^{(-)}\ u\bar{u} + c_{ns}^{(-)}\ d\bar{d} + c_s^{(-)}\ s\bar{s} \\ f_0\ (980) &\sim c_{ns}^{(+)}\ u\bar{u} + c_{ns}^{(+)}\ d\bar{d} + c_s^{(+)}\ s\bar{s} \end{aligned} \tag{58}$$

with normalization $2\,|\,c_{ns}^{\pm}\,|^2 + |\,c_s^{\pm}\,|^2 = 1$. We retain *only* the approximate relations in (57) and, according to the mechanism 1. in the above list, we infer for the $f_0\ (980)$

$$\begin{aligned} &X_\omega \simeq 2\,|\,c_{ns}\,|^2 \quad ; \quad X_\varphi \simeq |\,c_s\,|^2 \\ &c_{ns} = c_{ns}^{(+)} = c_{ns}^{(-)} \quad ; \quad c_s = c_s^{(+)} = c_s^{(-)}. \end{aligned} \tag{59}$$

The second equation in (57) is satisfied if we choose $c_s = 2c_{ns}$. Then we find for the vector $\mathbf{c} = (\ c_{ns}\ ,\ c_{ns}\ ,\ c_s\ )$[6] in case of $f_0\ (980)$

$$f_0\ (980): \qquad \mathbf{c} = \frac{1}{\sqrt{6}}\ (\ 1\ ,\ 1\ ,\ 2\ ) \tag{60}$$

and in case of $f_0\ (1500)$ accordingly the orthogonal composition

$$f_0\ (1500): \qquad \mathbf{c}\,' = \frac{1}{\sqrt{3}}\ (\ 1\ ,\ 1\ ,\ -1\ ). \tag{61}$$

These derivations reveal – within the approximations adopted – the pair $\eta\,'\ (958)$ and $f_0\ (980)$ as a *genuine* parity doublet. Thus $\eta\ \eta'$ and $f_0\ (980)\ f_0\ (1500)$ are related and governed approximately by the same singlet-octet mixing angle

$$\Theta \approx \arcsin\ 1/3\ = 19.47^{\rm o} \tag{62}$$

with respect to the vectors $\mathbf{e}_0 = \frac{1}{\sqrt{3}}\ (\ 1\ ,\ 1\ ,\ 1\ )$ and $\mathbf{e}_8 = \frac{1}{\sqrt{6}}\ (\ 1\ ,\ 1\ ,\ -2\ )$

$$\mathbf{c} = \mathbf{e}_0\ \cos\ \Theta\ -\ \mathbf{e}_8 \sin\ \Theta. \tag{63}$$

There is one difference though in the mass patterns of the two octets in that the $I = 0$ state closer to the octet is the lighter one in the pseudoscalar case (η) but the heavier one in the scalar case $(f_0\ (1500))$; then we adopt the following correspondence in the quark compositions (60) and (61)

$$\eta \quad \leftrightarrow \quad f_0(1500) \qquad \text{and} \qquad \eta' \quad \leftrightarrow \quad f_0(980). \tag{64}$$

With this flavor composition of the $f_0(1500)$ we also predict the ratio of decay widths

$$R = \frac{B(J/\psi\ \to\ \varphi\ f_0(1500))}{B(J/\psi\ \to\ \omega\ f_0(1500))} = \frac{1}{2} \tag{65}$$

[4] We are indebted to C. Greub for pointing out that the relevant decay modes of J/ψ comprise both φ *and* ω.

[5] We neglect here the phase space effects of $\lesssim 15\%$ whereby it is assumed that for the momenta $p \sim 1$ GeV the threshold behaviour of the P-wave is reduced to that of the S-wave by formfactors.

[6] The "mnemonic" approximate form of $\mathbf{c}$ is due to H. Fritzsch.

Table 7. Amplitudes for the decays into two pseudoscalar mesons of states with flavor mixing as in (66), using for the $f_0(980)$, the $f_0(1500)$ and the glueball the mixing angles $\sin\phi = \sqrt{2/3}$, $\sin\phi = -\sqrt{1/3}$ and $\sin\phi = \sqrt{1/3}$ respectively. The $\eta - \eta'$ mixing is according to (60) and (61), S denotes the relative $s\bar{s}$ amplitude. Normalization is to $\pi^+\pi^-$, the first row also indicates after ($\rightarrow$) the relative weights of $\pi\pi$ decays. For identical particles the width has to be multiplied by 1/2

channel	$q\bar{q}$ decay (ϕ)	$f_0(980)$	$f_0(1500)$	glueball
$\pi^0\pi^0$	$1 \rightarrow \cos\ \phi/\sqrt{2}$	$1 \rightarrow 1/\sqrt{6}$	$1 \rightarrow 1/\sqrt{3}$	$1 \rightarrow 1/\sqrt{3}$
$\pi^+\pi^-$	1	1	1	1
K^+K^-	$(\sqrt{2}\tan\phi + S)/2$	$(2+S)/2$	$(-1+S)/2$	$(1+S)/2$
$K^0\overline{K^0}$	$(\sqrt{2}\tan\phi + S)/2$	$(2+S)/2$	$(-1+S)/2$	$(1+S)/2$
$\eta\eta$	$(2+\sqrt{2}S\tan\phi)/3$	$2(1+S)/3$	$(2-S)/3$	$(2+S)/3$
$\eta\eta'$	$(\sqrt{2}-2S\tan\phi)/3$	$\sqrt{2}(1-2S)/3$	$\sqrt{2}(1+S)/3$	$\sqrt{2}(1-S)/3$
$\eta'\eta'$	$(1+2\sqrt{2}S\tan\phi)/3$	$(1+4S)/3$	$(1-2S)/3$	$(1+2S)/3$

which is inverse to the corresponding ratio for $f_0(980)$. A measurement of this ratio would be an interesting test of our hypotheses.

4.2 Mass pattern and Gell-Mann-Okubo formula

We come back to the two extremal possibilities for mixing discussed in Sect. 2.2 within the context of the σ model:

I) quenched singlet octet mixing,
II) strict validity of the OZI rule.

We now conclude, that the $q\bar{q}$ scalar nonet is nearer to case (I). Furthermore, we suggest a definite deviation from I) parametrized by the *approximate* mixing angle (62), the same as found for the pseudoscalar nonet.

This conclusion identifies the scalar nonet as second one – besides its pseudoscalar partner – showing a large violation of the OZI-rule.

Next we compare these results with the expected mass pattern as discussed in Sect. 2.2. In case of quenched singlet octet mixing (case I) one predicts from the Gell-Mann-Okubo mass formula for the members of an octet the heavier scalar $I = 0$ member to appear in the mass range 1550-1600 MeV, if one takes the a_0 and K_0^* masses as input. The deviation from the observed mass of the $f_0(1500)$ is 7-14% in the masses squared which we consider as tolerable; the deviation is attributed to effects of $O(m_s^2)$. Then the $f_0(980)$ is close to the singlet member of the nonet.

On the other hand, for a splitting according to the OZI rule the isoscalar $s\bar{s}$ state would be expected at the mass of ∼1770 MeV. In this case the $f_0(980)$ would be a purely non-strange state which is hardly consistent with the large decay rate $J/\psi \rightarrow \varphi f_0(980)$ in Table 6.

4.3 Decays into $\pi\pi$, $K\overline{K}$, $\eta\eta$ and $\eta\eta'$

These 2-body decays are again sensitive to the flavor composition of the $J^{PC} = 0^{++}$ particles. For further analysis we consider the decay of a $q\bar{q}$ state with arbitrary flavor composition where we define the mixing angle ϕ now with respect to the strange non-strange directions

$$q\bar{q} = n\overline{n}\ \cos\phi + s\bar{s}\ \sin\phi; \qquad n\overline{n} = (u\bar{u} + d\bar{d})/\sqrt{2}. \tag{66}$$

The decay amplitudes are calculated with flavor symmetry but the relative amplitude S to adjoin an $s\bar{s}$ pair relative to a nonstrange $u\bar{u}$ or $d\bar{d}$ one is assumed to deviate from symmetry. We assume S to be real with $0 \leq S \leq 1$ and $S \sim \frac{1}{2}$, but it may depend also on the mass of the decaying system with a restoration of symmetry at high energies. For a mixed state as in (66) this ansatz leads to the decay amplitudes in Table 7 which agree with the results in [92]. Here we take the decomposition of η and η' as in (60) and (61) with (64).[7] We also give the prediction for the two f_0 states with the same mixing as in the pseudoscalar sector as discussed above and for the glueball taken as colour singlet state.[8] We now examine how the predictions from our hypotheses on the flavor decomposition in Table 7 compare with experiment.

Couplings of the $f_0(980)$

This state has a mass near the $K\overline{K}$ threshold. So the directly measurable quantities are the reduced widths Γ_{red} into $\pi\pi$ and $K\overline{K}$ for which we predict according to Table 7

$$R_0 = \frac{\Gamma_{red}(f_0(980) \rightarrow K\overline{K})}{\Gamma_{red}(f_0(980) \rightarrow \pi\pi)} = \frac{(2+S)^2}{3} \tag{67}$$

The experimental determination from elastic and inelastic $\pi\pi$ scattering is difficult because of the unitarity constraints near the $K\overline{K}$ threshold. This can be avoided in a measurement of reaction (39a) at larger momentum transfer t where the $f_0(980)$ appears as a rather symmetric peak without much coherent background as already emphazised. Binnie et al. [61] used their data on the $\pi^+\pi^-$,

[7] For an analysis with $S = 1$, see also [15].

[8] Contrary to [92] we assume that the creation of quarks from the initial gluonic system is flavor symmetric and that the s-quark suppression occurs only in the secondary decay by creation of a soft $q\bar{q}$ pair.

Table 8. The ratio R_0 defined in (67) as determined from experiment and predicted for different strange quark amplitudes S

	exp. results		$S=0$	$S=0.5$	$S=1.0$
R_0	1.9 ± 0.5	Binnie [61]	1.3	2.1	3.0
	$\simeq 0.85$	MP [42]			

$\pi^0\pi^0$ and K^+K^- channels with $|t| \gtrsim 0.3$ GeV to measure the ratio (67) directly by fitting their distributions to the Breit-Wigner formula

$$\sigma_{\pi,K} \propto \left| \frac{\Gamma_{\pi,K}^{1/2}}{m_0 - m - i(\Gamma_\pi + \Gamma_K)/2} \right|^2 , \qquad (68)$$

where $\sigma_{\pi,K}$ denote the cross sections in the $\pi\pi$ and $K\overline{K}$ channels, respectively. Furthermore, $\Gamma_\pi = \gamma_\pi p_\pi$ and $\Gamma_K = g_K p_{K^+} + g_K p_{K^0}$, where p_h are the momenta of h in the hh *cms*. The reduced widths are given by $\Gamma_{red,\pi} = \gamma_\pi$ and $\Gamma_{red,K} = 2g_K$. We enter the result by Binnie et al. into Table 8. We also show the result of the fits by Morgan and Pennington (MP) [42] to $\pi\pi$ and $K\overline{K}$ final states from various reactions taking into account the coherent background and unitarity constraints. As we are close to the $K\overline{K}$ threshold the S parameter may be not well defined, this leaves a range of predictions also presented in Table 8. We see that the determination by Binnie et al. is comparable to the theoretical expectation whereas the one by MP (given without error) comes out a bit smaller.

We want to add that the determination of this ratio R_0 needs data on the $K\overline{K}$ process. The sensitivity to g_K in the denominator of (68) is very weak. Therefore from fits to the $\pi\pi$ spectra alone conflicting results are obtained.

Couplings of the $f_0(1500)$

With respect to the branching fractions of the $f_0(1500)$ into two pseudoscalars we scrutinize the phase space corrected reduced rate ratios deduced by C. Amsler [93]

$$R_1 = \frac{\Gamma_{red}\,(\,\eta\,\eta\,)}{\Gamma_{red}\,(\,\pi\,\pi\,)},$$
$$R_2 = \frac{\Gamma_{red}\,(\,\eta\,\eta^{'}\,)}{\Gamma_{red}\,(\,\pi\,\pi\,)},$$
$$R_3 = \frac{\Gamma_{red}\,(\,K\,\overline{K}\,)}{\Gamma_{red}\,(\,\pi\,\pi\,)} \qquad (69)$$

where all charge modes of $\pi\pi$ and $K\overline{K}$ are counted. The experimental determinations [93] are presented in Table 9. Using our amplitudes for the decays of the $f_0(1500)$ in Table 7 we predict for these ratios

$$R_1 = \frac{4}{27}\,(\,1 - \frac{1}{2}\,S\,)^2\,,$$
$$R_2 = \frac{4}{27}\,(\,1 + S\,)^2\,,$$
$$R_3 = \frac{1}{3}\,(\,1 - S\,)^2\,. \qquad (70)$$

Table 9. Reduced rate ratios R_i as defined in (69): experimental determinations by Amsler [93] and predictions for different strange quark amplitudes S according to (70)

ratio	data	$S = 0.352$	$S = 0.5$
R_1	0.195 ± 0.075	0.101	0.083
R_2	0.320 ± 0.114	0.271	0.333
R_3	0.138 ± 0.038	0.140	0.083

A χ^2 fit for S using the "data" in Table 9 yields

$$S = 0.352\ ^{+0.131}_{-0.109} \qquad (71)$$

with a satisfactory $\chi^2 = 0.887$ (for n.d.f. = 2). The range of values for S obtained in the fit as well as the reasonable agreement with the derived rates in [93] is compatible with the (approximately) identical mixing of *both* scalar and pseudoscalar nonets according to our assignments.

In particular we should note the large rate R_2 for the $\eta\eta^{'}$ decay mode, which strengthens the octet assignment of the $f_0(1500)$ (for a flavor singlet – the glueball in Table 7 – this decay mode would disappear in the flavor symmetry limit $S = 1$). On the other hand, the ratio R_3 is rather small which is in contradiction to a pure $s\overline{s}$ assignment looked for in some classification schemes. The smallness of R_3 is now naturally explained by the negative interference between the nonstrange and strange components of the $f_0(1500)$ in Table 7 which would actually be fully destructive in the $SU(3)_{fl}$ symmetry limit.

4.4 Decays into two photons

In this paragraph we focus first on the $f_0(980)$, which according to our hypotheses is a $q\overline{q}$ resonance (mainly). We distinguish the $q\overline{q}$ compositions of f_0 again according to the two cases I) – dominantly singlet – and II) – nonstrange – discussed before and include the third alternative – $f_0 \sim \overline{s}s$ – denoted T) , historically in the foreground, as proposed again recently by Törnqvist [32]. For the decay into two photons we compare with the neutral component of the isotriplet $a_0(980)$.

Disregarding sizable glueball admixtures to f_0 the decay amplitude to two photons becomes proportional to the characteristic factor well known from the corresponding decays of π^0, η, $\eta^{'}$ involving the quark charges in units of the elementary one and proportional to the number of colors; for a state with quark composition $(c_u,\ c_d,\ c_s)$ one obtains

$$S_{\gamma\gamma} = 3 \sum_{q=u,d,s} c_q\, Q_q^{\,2}. \qquad (72)$$

Then we obtain for the ratio of the two photon decay widths of f_0 and a_0 with (practically) the same phase

Table 10. Two photon branching ratio $R_{\gamma\gamma}$ defined in (73) for different mixing schemes according to the quark composition c_q

case		c_u	c_d	c_s	$R_{\gamma\gamma} = 2\,S^2_{\gamma\gamma}$
$f_0(980)$	(Ia) no mixing	$\frac{1}{\sqrt{3}}$	$\frac{1}{\sqrt{3}}$	$\frac{1}{\sqrt{3}}$	$\frac{24}{9} = 2.67$
	(Ib) $\eta - \eta'$ mixing	$\frac{1}{\sqrt{6}}$	$\frac{1}{\sqrt{6}}$	$\frac{2}{\sqrt{6}}$	$\frac{49}{27} = 1.815$
	(II) OZI-mixing	$\frac{1}{\sqrt{2}}$	$\frac{1}{\sqrt{2}}$	0	$\frac{25}{9} = 2.78$
	(T) pure $s\bar{s}$	0	0	1	$\frac{2}{9} = 0.22$
$a_0(980)$		$\frac{1}{\sqrt{2}}$	$-\frac{1}{\sqrt{2}}$	0	1

space

$$R_{\gamma\gamma} = \frac{\Gamma\,(f_0\,(980) \rightarrow \gamma\gamma\,)}{\Gamma\,(a_0\,(980) \rightarrow \gamma\gamma\,)}\,; \qquad R_{\gamma\gamma} = 2\,S^2_{\gamma\gamma}. \tag{73}$$

The predictions for the various mixing schemes are given in Table 10.

The Particle Data Group gives for the $a_0(980)$ and the $f_0(980)$

$$\Gamma\,(\,a_0 \rightarrow \gamma\gamma\,) = \left(\,0.24\,^{+0.08}_{-0.07}\,\right)\ \text{keV}\ /\ B(\,a_0 \rightarrow \eta\pi\,)$$
$$\Gamma\,(\,f_0 \rightarrow \gamma\gamma\,) = (\,0.56 \pm 0.11\,)\ \text{keV} \tag{74}$$

and therefore

$$R_{\gamma\gamma} = (\,2.33 \pm 0.9\,)\,B(a_0 \rightarrow \eta\pi\,). \tag{75}$$

The branching fraction $B(\,a_0 \rightarrow \eta\pi\,)$ is not determined satisfactorily because of conflicting analyses by Bugg et al. [94] , Corden et al. [95] and Defoix et al. [96], but the PDG classifies the $\eta\pi$ mode as "dominant".

We conclude from the measurement in (75) that case (T) with pure $\bar{s}s$ composition of $f_0(980)$ is untenable. On the other hand, it becomes obvious that a distinction between alternatives (Ia), (Ib) and (II) by these measurements would need a considerable increase in experimental precision.

Finally, we derive the corresponding prediction for the $f_0(1500)$ assuming its $q\,\bar{q}$ composition according to (61), identical to its η pseudoscalar counterpart. Concerning the deviations from the Gell-Mann-Okubo mass square formula in (32) we refer to the well known stability of the corresponding relation for the pseudoscalar nonet, with similar singlet octet mixing angle.

We obtain for the ratio of decay widths into 2 γ

$$R'_{\gamma\gamma} = \frac{\Gamma\,(\,f_0\,(1500) \rightarrow \gamma\gamma)}{\Gamma\,(\,f_0\,(980) \rightarrow \gamma\gamma\,)} \tag{76}$$

and the individual decay width of the f_0 (1500) the following predictions

$$R'_{\gamma\gamma} = \frac{32}{49}\left(\frac{m\,(\,f_0\,(1500)\,)}{m\,(\,f_0\,(980)\,)}\right)^p$$
$$\Gamma\,(f_0\,(1500) \rightarrow \gamma\gamma\,) \sim 0.3\,(\,0.1 \ldots 0.6\,)\ \text{keV}. \tag{77}$$

In Born approximation the power in (77) would be $p = 3$ and this power seems appropriate for the light pseudoscalars. At the higher energies, formfactor effects (typically[9] $p = -3$) become important. In (77) we give our best estimate, the lower limit corresponds to $p = -3$, the upper one corresponds to simple phase space with $p = 1$.

The branching ratios into two photons have also been considered in the model by Klempt et al. [34]. Their $f_0(1500)$ with mixing angle $\sin\phi = -0.88$ is very close to the octet state ($\sin\phi = -0.82$), yet closer than in our phenomenological analysis with $\sin\phi = -0.58$. Then they obtain for the above ratio $R'_{\gamma\gamma} \sim 0.086$. The results depend strongly on the mixing angle as $R'_{\gamma\gamma}$ has a nearby zero at $\sin\phi = -0.96$, corresponding to the mixture $(1,\ 1,\ -5)/\sqrt{27}$. For a pure octet assignment we would obtain $\Gamma \sim 0.08(0.03 \ldots 0.17)$ keV instead of (77).

It appears possible, that the 2 γ mode of f_0 (1500) can be detected in the double Bremsstrahlung reaction $e^+\,e^- \rightarrow e^+\,e^-\,f_0$ (1500). A first search by the ALEPH collaboration at LEP [97] did not show any $f_0(1500)$ signal. However, no clear signal of $f_0(980)$ has been observed either although this process is well established. It appears that the statistics is still too low. Also other decay modes such as $\eta\eta$ and $K\overline{K}$ of the f_0 (1500) look promising to be studied.

4.5 Relative signs of decay amplitudes

Besides the branching ratios of the states into various channels the relative signs of their couplings is of decisive importance. They can also be deduced from Table 7. The S-wave phases discussed in Sect. 3 in the mass range above 1 GeV are determined with respect to the phase of the leading $f_2(1270)$ resonance which is a nearly non-strange $q\bar{q}$ state. In this case ($\phi \approx 0$) the coupling to all decay channels in Table 7 is positive.

For the states discussed here we obtain the signs in Table 11. The predictions for the $f_0(1500)$ are in striking agreement with the data on inelastic $\pi\pi$ scattering discussed in the previous section, as can be seen from Fig. 4. The resonance loop in the $K\overline{K}$ channel is oriented "downwards" in opposite direction to the one in $\eta\eta$ and also opposite to the $f_2(1270)$ resonance defined as "upward". This is consistent with our assignment $(1, 1, -1)/\sqrt{3}$ in (61) for the $f_0(1500)$. It is not consistent in particular with the expectations for a glueball which would have positive couplings to all decay channels.

As for the other two states in Table 11 we have only the small window above the $K\overline{K}$ threshold. The amplitude in this region is composed of the tail of the $f_0(980)$ and the "background", i.e. the supposed glueball state according to our hypothesis. We note that in both channels the amplitude has a qualitatively similar behaviour in accord with the expected positive signs of all components.

[9] The transition amplitude should contain the nonperturbative constant $\langle 0|\bar{q}q|f_0\rangle = m_0^2$, then $p = -3$ follows for dimensional reasons. Experimental data on the $\gamma\gamma$ decays of the tensor mesons are consistent with $p \sim -3$ assuming ideal mixing.

Table 11. Signs of amplitudes for the decays of scalar states into $K\overline{K}$ and $\eta\eta$ relative to the $f_2(1270)$

decay	$f_0(980)$	$f_0(1500)$	glueball
$K\overline{K}$	+	−	+
$\eta\eta$	+	+	+

At present we have no quantitative model for the absolute phase around 230° for the superposition of these two states.

5 The lightest glueball

Adopting the *phenomenological hypotheses* a) - c) in Sect. 1 we have exhausted in the previous analysis all positive parity mesons in the PDG tables below 1600 MeV with the *notable* exception of the scalar $f_0(400-1200)$ and also the $f_0(1370)$ which we did not accept as standard Breit-Wigner resonance. We consider the spectrum in Fig. 3 (the "red dragon") with the peaks around 700 and 1300 MeV and possibly with another one above 1500 MeV as a reflection of a single very broad object ("background") which interferes with the f_0 resonances. In elastic $\pi\pi$ scattering this "background" is characterized by a slowly moving phase which passes through 90° near 1000 MeV if the $f_0(980)$ is subtracted (see, for example [42]). This "background" with a slowly moving phase is also observed in the 1300 MeV region in the inelastic channels $\pi\pi \to \eta\eta,\ K\overline{K}$ as discussed above. It is our hypothesis that this very broad object which couples to the $\pi\pi$, $\eta\eta$ and $K\overline{K}$ channels is the lightest glueball

$$f_0(400-1200),\ f_0(1370) \to gb_0(1000) \qquad (78)$$
$$\Gamma[gb_0(1000)] \sim 500-1000 \text{ MeV}.$$

The large width is suggested by the energy dependent fits in Table 4. From the speed of the phase shift δ_0^0 near 1000 MeV – $\frac{d\delta_0^0}{dm} \simeq 1.8$ GeV^{-1} after the $f_0(980)$ effect has been subtracted out as in [42] – one finds using (48) the larger value $\Gamma(gb_0) \sim 1000$ MeV. The glueball mass (78) corresponds to alternative 1) ($m_{gb_0,\infty} \lesssim m_{a_0} \sim 1$ GeV) as described at the beginning of Sect. 2.

We do not exclude some mixing with the scalar nonet states but it should be sufficiently small such as to preserve the main characteristics outlined in the previous section. In the following we will investigate whether our glueball assignment for the states in (78) is consistent with general expectations.

5.1 Reactions favorable for glueball production

We first examine the processes in which particles are expected to be produced from gluonic intermediate states.
(a) $pp \to pp\ +\ X_{\text{central}}$
In this reaction the double pomeron exchange mechanism should be favorable for the production of gluonic states. A prominent enhancement at low $\pi\pi$ energies is observed [70,71] and can be interpreted in terms of the elastic $\pi\pi$ phase shifts [41,42].
(b) Radiative decays of J/ψ
For our study of scalars the most suitable final states are those with the odd waves forbidden. The simplest case is $J/\psi \to \gamma\pi^0\pi^0$ which has been studied by the Crystal Ball Collaboration [98]. The mass spectrum shows a prominent $f_2(1270)$ signal but is sharply cut down for masses below 1000 MeV and the presentation ends at $m_{\pi\pi} \sim 700$ MeV. This cutoff in the mass spectrum is not due to the limited detector efficiency which is flat over the full mass region down to ~ 600 MeV and drops sharply only below this mass value [99].

An incoherent background is fitted in [98] under the f_2 peak which reaches the fraction 1/7.5 at the maximum of the peak. This is not much smaller than 1/(5+1) expected for the S-wave from the counting of spin states. No data have been presented on the azimuthal angle distribution which would allow to estimate the amount of S-wave. No further hint can be obtained from the $\pi^+\pi^-$ channel analysed by the Mark III collaboration [101] because of the larger background.

It appears that – contrary to our expectation – there is no low mass enhancement around 700 MeV in this channel related to the glueball; its production with higher mass of around 1300 MeV is not inconsistent with data. For the moment we have no good explanation for the low mass suppression.
(c) Transition between radially excited states.
The radially excited states ψ', Y' and Y'' can decay by two gluon emissions into the heavy quark ground state and give therefore rise to the production of gluonic states. The observed $\pi\pi$ mass spectra can be described consistently using the elastic $\pi\pi$ S-wave phase shifts [41] although the calculation is not very sensitive to their detailed behaviour. Another example of this kind is the decay of the $\pi(1300)$, presumably a radial excitation of the stable π; its decay mode into $(\pi\pi)_{S-wave}\pi$ is seen [102].
Finally, we comment on the different production phases of the glueball amplitude with respect to the $f_0(980)$ discussed in Sect. 3.3. In most inelastic reactions the $f_0(980)$ appears as peak above the background (case b) which is consistent with the phases of the decay amplitudes for this state and the glueball to be the same as expected from Table 7. The dip occurs in elastic scattering (case a) where a peak is not allowed as the background is already near the unitarity limit. In two reactions (case c) the large asymmetry in the mass spectra suggests a background out of phase by 90° with respect to the $f_0(980)$ Breit-Wigner amplitude which may be a hint to different production phases.

5.2 Flavor properties

Here we list a few observations which may give a hint towards the flavor composition along the lines discussed for the $q\overline{q}$ nonet.

Glueball production in $p\bar{p}$ annihilation
The Crystal Barrel Collaboration has observed the $f_0(1370)$ in the processes

$$p\overline{p} \;\rightarrow\; f_0(1370)\;\pi^0; \quad f_0(1370) \;\rightarrow\; K_L K_L,\; \eta\eta \qquad (79)$$

where clear peaks in the respective mass spectra have been seen. The theoretical expectation for the ratio of reduced branching ratios assuming $f_0(1370)$ to decay like a glueball according to Table 7 is obtained as

$$R_g \;=\; \frac{\Gamma_{red}(f_0(1370)\rightarrow\eta\eta)}{\Gamma_{red}(f_0(1370)\rightarrow K\overline{K})} \;=\frac{(2+S)^2}{9(1+S)^2}. \qquad (80)$$

From the results summarized by Amsler [93] we derive the quantity (80) after correction for phase space and unseen $K\overline{K}$ decay modes

$$\text{exp. result}: \qquad R_g \;\sim 0.44. \qquad (81)$$

This number is to be compared with the theoretical expectations for different strange quark amplitudes S

$$\text{theor. result}: \qquad S=(0,\;0.5,\;1.0): \qquad R_g=(0.44,\;0.31,\;0.25). \qquad (82)$$

The value extracted from the measurements is somewhat larger than expected but looking at the difficulty to extract such numbers experimentally we consider the result as encouraging. Similar results for the $f_0(400-1200)$ cannot be extracted from the data in [93] because of the overlap with nearby other states.

J/psi decay into glueball + vector mesons
In analogy with the flavor analysis of the f_0 states above we now proceed with our glueball candidate. In the final state $\phi\pi\pi$ DM2 observes indeed a broad background under the $f_0(980)$ which extends towards small masses in the $\pi\pi$ invariant mass [64]. On the other hand the mass spectrum in the final state $\omega\pi\pi$ looks very different with a peak at low masses around 500 MeV [66]. Similar results are also seen by Mark-III [65].

If the low mass bump in the $\omega\pi\pi$ final state is a real effect and not due to background[10] it requires quite a different dynamics in the two vector meson channels. One possibility is the suppression of low mass $\pi\pi$ pairs from the decay of an $s\bar{s}$ pair because of the heavier s-quark mass. This problem could be avoided by a restriction of the comparison to the mass region above 1 GeV.

5.3 Suppressed production in $\gamma\gamma$ collisions

If the mixing of the glueball with $q\bar{q}$ states is small then the same is true for the two photon coupling. We consider here the processes

$$\text{(a)}\quad \gamma\gamma\rightarrow\pi^+\pi^- \qquad \text{(b)}\quad \gamma\gamma\rightarrow\pi^0\pi^0. \qquad (83)$$

[10] In [65] the important background from $\phi\eta,\ \eta\rightarrow 2\pi+\pi^0$ has been emphasized; it could also appear in the ω channel

and distinguish two regions for the mass $W\equiv m_{\pi\pi}$.

Low energies $W\lesssim 700\ MeV$
The process (a) is dominated by the Born term with pointlike pion exchange. This contribution is avoided in process (b) and the remaining cross section is smaller by one order of magnitude in the same mass range; furthermore, it is also very small compared to the dominant cross section at the $f_2(1270)$ resonance position. The reaction (b) has been studied by the Crystal Ball [67] and JADE [69] Collaborations.

We compare the cross section in $\gamma\gamma\rightarrow\pi^0\pi^0$ and in the isoscalar elastic $\pi\pi$ scattering near the peak at $W\sim 600$ MeV. Only in the second reaction the glueball should have a sizable coupling. We normalize both cross sections to the $f_2(1270)$ meson peak representing a well established $q\bar{q}$ state and obtain

$$R_\gamma = \frac{\sigma_{\gamma\gamma}(W_1=600\text{ MeV})}{\sigma_{\gamma\gamma}(W_2=1270\text{ MeV})} \simeq 0.067 \qquad (84)$$

$$R_\pi = \frac{\sigma^S_{\pi\pi}(W_1=600\text{ MeV})}{\sigma^D_{\pi\pi}(W_2=1270\text{ MeV})} \;=\; \frac{1}{5x_f}\frac{W_2^2}{W_1^2} \simeq 1.05. \qquad (85)$$

Here we used for R_γ the data from [67] and for the $\pi\pi$ S-wave the cross section at the unitarity limit and the same for the f_2 meson in the D-wave but with elasticity $x_f=0.85$. The ratios in (85) demonstrate that the low mass S-wave production in $\gamma\gamma$ collisions is suppressed by more than an order of magnitude in comparison to $\pi\pi$ collisions.

The size of the cross sections in both charge states in (83) can be understood [67,103] by including the Born term in (a) only and a rescattering contribution in both processes. So one can interpret the reaction (b) as a two step process, first the two photons couple to charged pions as in (a) then rescattering by charge exchange $\pi^+\pi^-\rightarrow\pi^0\pi^0$: in this picture the photons do not couple "directly" to the "quark or gluon constituents" of the broad structure at 600 MeV but only to the initial charged pointlike pions. This is at the same time a minimal model for the production of the bare glueball according to our hypothesis without direct coupling of the photons to the glueball state.

Mass region around the $f_2(1270)$
One may look again for the presence of an S-wave state. The measurement of the angular distribution does not allow in general a unique separation of the S-wave from the D_λ-waves in helicity states $\lambda=0$ and $\lambda=2$. It turns out, however, that the data are best fitted in the mass region $1.1\le W\le 1.4$ GeV by the D_2 wave alone without any S and D_0 wave included [67–69]. A restriction on the spin 0 contribution has been derived at the 90% confidence limit in [67] as

$$\frac{\sigma_{\gamma\gamma}(\text{spin }0)}{\sigma_{\gamma\gamma}(\text{total})} \;<\; 0.19 \quad \text{for} \quad 1.1\;\le\; W\;\le\; 1.4\text{ GeV} \qquad (86)$$

which turns out not yet very restrictive. Taking all three experiments together a suppression of S wave under the $f_2(1270)$ is suggested.

In summary, the production of the broad S-wave enhancement is suppressed in $\gamma\gamma$ in comparison to $\pi\pi$ collisions, and this is very clearly seen at the low energies. This we consider as a strong hint in favor of our hypothesis of the mainly gluonic nature of this phenomena both at low and high energies. Clearly, the study of scalar states in $\gamma\gamma$ collisions will be of crucial importance for the determination of their flavor content and classification into multiplets.

5.4 Quark-antiquark and gluonic components in $\pi\pi$ scattering

In our picture, the elastic $\pi\pi$ scattering amplitude in the energy region below ~ 2 GeV is not saturated by $q\overline{q}$ resonances in the s- and t-channel alone.[11] There is a second component which corresponds to Pomeron exchange in the t-channel – dual to the so-called "background" in the s-channel. This dual picture with two components, suggested by Freund and Harari [107], has been very successful in the interpretation of the πN scattering data.

In case of the $\pi\pi$-interaction a similar situation was found by Quigg [108]: whereas the $I_t = 1$ t-channel exchange amplitude can be saturated by $q\overline{q}$ resonances, the $I_t = 0$ amplitude obtains a contribution of about equal magnitude from the "background" as well. This background is present already in the low energy region around 1 GeV and is seen clearly in the S-wave amplitude corresponding to $I_t = 0$ [108]; it also governs the exotic $\pi^+\pi^+$ channel.

The Pomeron exchange is naturally related to glueball exchange. Then, we consider a third component, obtained by crossing, with glueball intermediate states in the s-channel and exotic four quark states in the t-channel. Indeed, the $\pi\pi$ $I_t = 2$ exchange amplitude in [108] shows resonance circles with little background and therefore could correspond to a glueball amplitude after appropriate averaging. This third component with exotic exchange is expected to drop yet faster with energy than the $q\overline{q}$ resonance exchange amplitude. We consider the phenomenological results on the low energy "background" [108] as a further independent hint towards a gluonic component in the low energy $\pi\pi$ scattering.

6 Completing the basic triplet of gauge boson binaries

After we found the candidate for gb (0^{++}) at ~ 1 GeV we expect, as discussed in Sect. 2, the two remaining members of the basic triplet with J^{PC} quantum numbers 0^{-+} and 2^{++} to be heavier than gb (0^{++}) and to exhibit a much smaller width because of the reduced strength of the interaction (coupling α_s) at higher mass

$$\begin{aligned} gb\ (0^{-+}):&\quad m_2 > 1\ \text{GeV}\ ,\quad \Gamma_2 \ll 1\ \text{GeV};\\ gb\ (2^{++}):&\quad m_3 \gtrsim m_2\ ,\qquad \Gamma_3 \ll 1\ \text{GeV}. \end{aligned} \tag{87}$$

Thus we are looking for two resonances, the width of which make them appear much more similar to their prominent, relatively narrow $q\,\overline{q}$ counterparts. The mass range is tentatively set to $1 - 2$ GeV.

We search for possible candidates in radiative J/ψ decay, on which we focus next. To this end we list in Table 12 the most prominent radiative decay modes of $J/\psi \to \gamma X$ into a single resonance X without charm content. Among the 5 resonances we recognize $\eta(1440)$ as a candidate for gb (0^{-+}) and $f_J(1710)$ with spin J either 0 or 2, as a candidate for gb (2^{++}).

Table 12. Radiative decay modes of J/ψ into single non-$c\overline{c}$ resonances with branching ratios $B \gtrsim 10^{-3}$ according to the PDG [18]

name (X)	$B(J/\psi \to \gamma X) \times 10^3$	partial B	mode
1 η' (958)	4.31 ± 0.30		
2 η (1440)	$> 3.01 \pm 0.44$		
		1.7 ± 0.4	$\varrho^0\varrho^0$
		0.91 ± 0.18	$K\overline{K}\pi$
		0.34 ± 0.07	$\eta\pi^+\pi^-$
		0.064 ± 0.014	$\gamma\varrho^0$
3 f_4 (2050)	2.7 ± 1.0		$\pi\pi$
4 f_2 (1270)	1.38 ± 0.14		$\pi\pi$
5 f_J (1710)	$0.85^{+1.2}_{-0.9}$		$K\overline{K}$

6.1 The glueball with $J^{PC} = 0^{-+}$

A state with these quantum numbers is expected to decay into 3 pseudoscalars (ps). The first experiments on the radiative decays $J/\psi \to \gamma\ 3\ ps$ were performed by the MarkII [109] and Crystal Ball [110] collaborations in the channels $3\ ps = K_sK^{\pm}\pi^{\mp}$ and $3\ ps = K^+K^-\pi^0$, respectively.

A spin analysis was performed by Crystal Ball [110]; it revealed a major intermediary decay mode

$$\eta(1440) \to a_0(980)\pi \to K\overline{K}\pi \tag{88}$$

and $J^{PC}[\eta(1440)] = 0^{-+}$. While the branching fraction product $B\,(\,J/\psi \to \gamma\eta\,(1440)\,) \times B\,(\eta\,(1440) \to K\overline{K}\pi)$ was overestimated in [109,110], the spin parity assignment was confirmed by Mark-III [111] in the decay mode

$$\eta(1440) \to a_0(980)\pi \to \eta\pi^+\pi^- \tag{89}$$

[11] This would follow with "one-component-duality" between direct channel resonances and t-channel Regge-poles as, for example, realized in the Veneziano model [104] or, alternatively, in resonance pole expansions in both channels simultaneously, as in [105], or, more recently, in [106].

and by DM2 [112] in both channels of (88) and (89). It is therefore natural to associate this state with its large radiative J/ψ decay mode with the 0^{-+} glueball.

On the other hand, in pp and πp collisions the central production of this state is weak in comparison to the leading $q\overline{q}$ resonances [113] or not resolved at all [13].

The glueball interpretation has a long history of debate [114,2]. Doubts have been brought up, in particular, in view of the results from lattice QCD calculations referred to in Sect. 2 which suggest a heavier mass above 2 GeV. As we discussed there, we feel that for a justification of such doubts, the more complete calculations should be awaited. However, because of the near absence in central production, the glueball interpretation is at a more speculative level at present.

6.2 The glueball with $J^{PC} = 2^{++}$

This state is expected to decay into two pseudoscalars. $f_J(1710)$ has long been a prime candidate. The problem for the classification of this state was and still is [18] the ambiguity in the spin assignment $J = 0$ or $J = 2$. In the following, we discuss the results of spin analyses in various experiments on J/ψ decays and central hadronic collisions which will lead us to a definite conclusion concerning the existence of a $J = 2$ state.

6.2.1 Radiative J/ψ decays

Crystal Ball experiment
The first observation of this state was obtained by the Crystal Ball collaboration at the SPEAR storage ring in '81 [100] in the decay channel

$$J/\psi \ \rightarrow \ \gamma \ \eta\eta. \tag{90}$$

The useful sample contained 50 events in the $\eta\eta$ invariant mass range from 1200 - 2000 MeV. The resonance parameters were [100]:

$$m \ = \ 1640 \ \pm \ 50 \text{ MeV} \quad , \quad \Gamma \ = \ 220 \ ^{+100}_{-70} \text{ MeV}. \tag{91}$$

A spin analysis with respect to the two hypotheses $J = 2$ and $J = 0$ was performed with at least statistical preference of $J^{PC} \ = \ 2^{++}$. The same resonance could not be resolved in a significant way by the same collaboration in the channel $J/\psi \ \rightarrow \ \gamma \ \pi^0\pi^0$ [98]. The scarcity of events is matched by the scarcity of precise description of the analysis.
Mark-III and DM2 experiments
A significant improvement in statistics is next reported by the Mark-III collaboration [101] in the channels

$$J/\psi \ \rightarrow \ \gamma \ \pi^+ \ \pi^-, \quad \gamma \ K^+ \ K^-. \tag{92}$$

We first discuss the results in the $\pi^+ \ \pi^-$ subchannel. The two resonances $f_2(1270)$ and $f_J(1710)$ are clearly resolved and a small indication of $f_2{}'(1525)$ is visible in the projected $\pi^+ \ \pi^-$ invariant mass distribution. A full exposition is given of the relevant angular acceptances and efficiencies. Now a fit of four interfering resonances is performed:

$$f_2 \ (1270) \ , \ f_2^{'} \ (1525) \ , \ f_J \ (1710) \ , \ f \ (2100).$$

The same reaction was investigated by the DM2 collaboration at the DCI storage ring in Orsay [115] with rather similar results. The product of branching ratios in both experiments is given as

$$\begin{aligned} &B(J/\psi \rightarrow \gamma f_2^{'}(1525)) \ \times \ B(f_2^{'}(1525) \rightarrow \pi^+\pi^-) : \\ &\text{Mark-III} : \sim \ 3 \times 10^{-5}; \\ &\text{DM2} : \ (2.5 \pm 1.0 \pm 0.4) \ 10^{-5} \end{aligned} \tag{93}$$

$$\begin{aligned} &B(J/\psi \rightarrow \gamma f_J(1710)) \ \times \ B(f_J(1710) \rightarrow \pi^+\pi^-) : \\ &\text{Mark-III} : \ (1.6 \pm 0.4 \pm 0.3) \ 10^{-4}; \\ &\text{DM2} : \ (1.03 \pm 0.16 \pm 0.15) \ 10^{-4} \end{aligned} \tag{94}$$

We remark that both experiments reveal a background of $O(20\%)$ in the $\pi^+\pi^-$ channel. This we expect to be – at least in part – not incoherent background, but the S-wave part, including the contribution from gb (0^{++}) discussed in the last section.

Next we turn to the K^+K^- channel with results again from Mark-III [101] and DM2 [116]. A full spin analysis is performed by the Mark-III collaboration for both invariant mass domains corresponding to $f_2^{'}(1525)$ and $f_J(1710)$. The likelyhood functions used to distinguish the two hypotheses $J = 0$ and $J = 2$ strongly favor the $J = 2$ hypothesis for both resonances. For the spin 0 assignment to $f_J(1710)$ the purely statistical probability is estimated to be 2×10^{-3} only. Especially the non-uniform polar angle distribution in the resonance decay requires the higher spin $J = 2$. This confirms the low statistics spin analysis of Crystal Ball [100].

No spin analysis is performed in this channel by DM2 in [116]. However, one can see from the Dalitz plot that the density of points along the $f_J(1710)$-band is peaked towards the edges, again favoring the presence of higher spin. Furthermore, in the projected K^+K^- invariant mass distribution an interference effect between the two resonances is visible, without any mention in [116]. Both phenomena, if analyzed and eventually confirmed, would yield an independent indication for the $J = 2$ quantum number of $f_J(1710)$.

The branching fraction products corresponding to (93) and (94) are determined as

$$\begin{aligned} &B(J/\psi \rightarrow \gamma f_2^{'} \ (1525)) \ \times \ B(f_2^{'}(1525) \rightarrow K^+K^-) : \\ &\text{Mark-III} : \ (3.0 \pm 0.7 \pm 0.6) \ 10^{-4}; \\ &\text{DM2} : \ (2.5 \pm 0.6 \pm 0.4) \ 10^{-4}. \end{aligned} \tag{95}$$

$$B(J/\psi \to \gamma f_J(1710)) \ \times \ B(f_J(1710) \to K^+K^-) :$$

$$\text{Mark-III}: \ (4.8 \pm 0.6 \pm 0.9)\ 10^{-4}; \qquad (96)$$

$$\text{DM2}: \ (4.6 \pm 0.7 \pm 0.7)\ 10^{-4}$$

From the branching fractions in (93) - (96) we obtain the following ratio in comparison with the PDG result:

$$\begin{aligned} \text{Mark-III and DM2}: \ & \frac{B(f_2^{'}(1525) \to \pi\pi)}{B(f_2^{'}(1525) \to K\overline{K})} \\ & = \ 0.075 \ \pm \ 0.030 \\ \text{PDG}: \ & = \ 0.0092 \pm \ 0.0018. \end{aligned} \qquad (97)$$

The obvious discrepancy between both numbers may point towards larger systematic errors in the relative efficiency of the two channels in (92) and eventually also to errors in the determinations of $f_2^{'}(1525)$ branching fractions in earlier experiments. However, we tend to believe that the discrepancy of deduced branching fractions in (97) is too significant to be "explained" by some unknown source of large errors; rather we conclude that *the peaks "$f_2^{'}(1525)$" as seen in radiative decays $J/\psi \ \to \ \gamma \ \pi^+\pi^-$, K^+K^- are not just $f_2^{'}(1525)$*. There are further states, in particular in the S-wave, which are not resolved in the analysis. One candidate is $f_0(1500)$, not yet established at the time of the Mark-III and DM2 experiments under discussion. Because of the small branching fraction of $f_0(1500)$ into $K\overline{K}$ deduced by Amsler [93], the effect is expected to be especially important in the $\pi\pi$ channel. Furthermore, there could be contributions from the high-mass tail of the 0^{++} glueball or other states in this partial wave. Such contributions may also affect the spin determinations of $f_J(1710)$.

Reanalysis of the $f_J(1710)$ spin by Mark-III

The spin analysis in the $K\overline{K}$ channel was subsequently extended by the Mark-III collaboration with higher statistics and including the K_sK_s final states [117,118]. In a mass-independent analysis, both the $J = 0$ and the $J = 2$ components have been studied, preliminary results became available as conference reports [119,120]. In these analyses the earlier Mark-III results [101] are contradicted in favor of a large $J = 0$ component of $f_J(1710)$, although a contribution of up to 25% from spin 2 was not excluded.

Looking into these results in more detail, we observe a considerable qualitative difference between the K^+K^- and the K_sK_s results. Whereas in the former channel the $J = 0$ component dominates over $J = 2$ by a factor 4.5 in the mass range 1600-1800 MeV, the opposite is true for the neutral kaon mode: in this case, the $J = 2$ component dominates by a factor 2.8 over $J = 0$. It is interesting to note that the efficiency in the azimuthal angle ϕ is much better in the neutral mode: for K^+K^- pairs the acceptance drops towards its minimum at $\phi = 0, \pi$ to $\sim$15% of its maximal value, but for K_sK_s pairs only to 57%. Therefore, the results from the neutral mode are very important despite the somewhat lower statistics.

Breit-Wigner resonance fits to the combined $K\overline{K}$ data sample are presented in Fig. 2a of [120]. In this data compilation, a significant spin 2 component of $f_J(1710)$ is clearly visible and is comparable in its overall size with the $f_2'(1525)$ signal. The fitted curve does not describe the data well near $f_J(1710)$ and underestimates the observed rates by roughly a factor of two. In view of the preliminary character of these studies, one might conclude that both hypotheses $J = 2$ and $J = 0$ should be considered.

BES experiment

The situation became considerably clarified by the recent results of the BES collaboration [121]. At the BEBC facility in Beijing, the decay $J/\psi \ \to \ \gamma \ K^+K^-$ was analyzed with specific determination of all helicity amplitudes for $J = 0, \ 2$. The region around 1700 MeV for the K^+K^- invariant mass spectrum – beyond $f_2^{'}(1525)$ – reveals a dominant resonant structure with spin 2. Furthermore, the analysis provides evidence indeed for a 0^{++} resonance, although weaker and less significant and at a slightly larger mass value. The parameters of the resonance fit are given in Table 13. The results on $f_2^{'}(1525)$ are now in good agreement with the PDG results. In comparison with the earlier results in (96) both the smaller branching ratios of $f_J(1710)$ into spin $J = 2$ alone and the reduced statistical errors are to be noted.

In comparison with the preliminary Mark-III results [120], we note the good agreement with their branching ratio into $f_2(1525)$ of $(1.7 \pm 0.3) \times 10^{-4}$ (for K^+K^- mode as defined in our Table 13). The corresponding fraction for $f_J(1710)$ with $J = 2$ reads $(1.0 \pm 0.4) \times 10^{-4}$ [120] – which we would increase by a factor 2 to $\sim 2.0 \times 10^{-4}$ as explained above – to be compared with $2.5{\times}10^{-4}$ in our Table 13. So there are no gross differences in the identification of the $J = 2$ objects in these experiments.

6.2.2 Hadronic decays $J/\psi \ \to \ \omega X \ ; \ \varphi X$

A new interesting chapter in studying hadronic J/ψ decays has been opened up by the Mark-III collaboration in the channels

$$J/\psi \ \to \ \gamma \ K\overline{K}; \quad \omega \ K\overline{K} \ \ ; \quad \varphi \ K\overline{K} \qquad (98)$$

discussed by L. Köpke [122]. The $K\overline{K}$ invariant mass distributions in the charge state K^+K^- in the three channels (98) are compared in Fig. 2 of [122].

In the $\omega \ K^+K^-$ channel the (mainly) $f_2^{'}(1525)$ signal – clearly visible in the other two decay modes in (98) – is absent. The most interesting channel is $\varphi \ K^+K^-$, where $f_J(1710)$ is visible only as a broadening shoulder of the dominant $f_2^{'}$ resonance. Köpke presents two fits to the acceptance/efficiency corrected invariant mass distributions, one admitting interference between $f_2^{'}(1525)$ and $f_J(1710)$ and one with incoherent addition of the two resonances. He shows, that only the coherent superposition admits to assign mass and width to $f_J(1710)$ compatible with the same parameters as determined in other channels. For angular integrated mass spectra the crucial consequence of coherent superposition is that the two resonances have to have the same spin. The quantitative dis-

Table 13. Resonance parameters from fit to mass regions near $f_2{}'(1525)$ and $f_J(1710)$ as obtained by the BES collaboration [121]

$J^{PC}(X)$	mass (MeV)	width (MeV)	$B\,(J/\psi \to \gamma X)$ $\times B\,(X \to K^+K^-) \times 10^4$
2^{++}	$1696 \pm 5\,^{+9}_{-34}$	$103 \pm 18\,^{+30}_{-11}$	$2.5 \pm 0.4\,^{+0.9}_{-0.4}$
2^{++}	$1516 \pm 5\,^{+9}_{-15}$	$60 \pm 23\,^{+13}_{-20}$	$1.6 \pm 0.2\,^{+0.6}_{-0.2}$
0^{++}	$1781 \pm 8\,^{+10}_{-31}$	$85 \pm 24\,^{+22}_{-19}$	$0.8 \pm 0.1\,^{+0.3}_{-0.1}$

tinction between the two fits is however not disclosed in [122].

Precisely this question is taken up by the DM2 collaboration [64]. Falvard et al. perform three fits, two with coherent superposition and one with incoherent superposition. The respective χ^2 (p.d.f.) clearly favor the two fits with coherence. We take these results together as further indication of a large spin $J = 2$ component in $f_J(1710)$.

6.2.3 Hadronic collisions

Central production
If $f_J(1710)$ is a glueball it should also be produced centrally in hadronic collisions. Indeed, the WA76 collaboration working with the Omega spectrometer [123] has observed a clear signal in the K^+K^- and K_sK_s mass spectra in

$$pp \to p_{fast}(K\overline{K})p_{slow} \tag{99}$$

at 85 and 300 GeV. Similar to the case of radiative J/ψ decays, two peaks appear above a smooth background from $f_2'(1525)$ and $f_J(1710)$. The polar angle decay distribution in both resonance regions is rather similar and largely non-uniform. It is concluded that the spin of $f_J(1710)$ is $J = 2$ and the assignments $J^P = 1^-$ and $J^P = 0^+$ are excluded.

Very recently, new results on reaction (99) at 800 GeV have been presented by the E690 collaboration at Fermilab [124]. In the region of interest, the mass spectrum again shows two peaks. Surprisingly, the first peak is now dominated by $f_0(1500)$ besides a smaller contribution presumably from $f_2(1525)$. Looking at the small branching ratio into $K\overline{K}$ (see Table 7) the process (99) could serve as a real $f_0(1500)$ factory if confirmed.

In the region of $f_J(1710)$, there are two solutions with large and small spin $J = 2$ component, respectively. No attempt has been made to find the most appropriate decomposition into Breit-Wigner resonances consistent with other knowledge. For the moment, the most accurate data leave us with a large uncertainty.
Peripheral production
Finally, we quote the work by Etkin et al. [84] measuring $\pi^- p \to K_sK_sn$ collisions which we discussed already before in Sect. 4 in connection with the $f_0(1500)$ state. In the higher mass region, the same experiment gave evidence of another scalar state at 1771 MeV and $\Gamma \sim 200$ MeV which is produced through the one pion exchange mechanism. It is natural to identify this state with the one observed in the $f_J(1710)$ region. The higher mass agrees well with the one observed by BES (see Table 13).

6.2.4 Summary on spin assignments to $f_J(1710)$

We summarize the experimental indications for both $J = 2$ and $J = 0$ in Table 14. The experiments in group (1) and (2), analyzing a single mass interval around 1700 MeV, all prefer $J = 2$ clearly over $J = 0$. The more refined experiments with higher statistics performing a mass-independent analysis find a spin zero component in addition. As a $J = 0$ state is found in peripheral collisions (3) in this mass range, it is most natural to associate it with a scalar quarkonium state $f_0(1770)$ MeV, slightly higher in mass than $f_J(1710)$. On the other hand, the prominent peak in the $J = 2$ wave only appears in the gluon-rich reactions (1) and (2), and is therefore our primary glueball candidate

$$J = 2: \qquad f_J\,(1710) \to\; gb\;(\;2^{++}\;) \tag{100}$$

which completes the basic triplet of binary glueballs.

7 Conclusions

In this paper we have reanalysed the spectroscopic evidence for various hadronic states with the aim to find the members of the $q\overline{q}$ nonet with $J^{PC} = 0^{++}$ of lowest mass and to identify the triplet of lightest binary glueballs. We draw the following conclusions from our study:

1. *The 0^{++} $q\overline{q}$ nonet*
   As members of this multiplet we identify the isoscalar states $f_0(980)$ and $f_0(1500)$ together with $a_0(980)$ and $K_0^*(1430)$. The mixing between the isoscalars is about the same as in the pseudoscalar nonet, i.e. little mixing between singlet and octet states, with the correspondence and approximate flavor decomposition $(u\overline{u}, d\overline{d}, s\overline{s})$

   $$\eta \leftrightarrow f_0(1500) \quad \tfrac{1}{\sqrt{3}}\,(1,\ 1,\ -1) \quad \text{close to octet},$$
   $$\eta' \leftrightarrow f_0(980) \quad \tfrac{1}{\sqrt{6}}\,(1,\ 1,\ 2) \quad \text{close to singlet},$$

   whereby the $(\eta',\ f_0(980))$ pair forms a parity doublet approximately degenerate in mass.

Table 14. Summary of spin assignments to the $f_J(1710)$ in the various analyses for three reaction types. The spin determination is carried out in a single mass bin (sb) or mass-independent analysis (mi)

Collaboration	$J = 2$	$J = 0$	channel	method
(1) J/ψ decays :				
Crystal Ball [100]	yes	no	$\gamma\ \eta\eta$	spin analysis (sb)
Mark-III [101]	yes	no	$\gamma\ K^+K^-$	spin analysis (sb)
Mark-III prel. [120]	$\sim 25\% - 40\%$	yes	$\gamma\ K\overline{K}$	spin analysis (mi)
BES [121]	75%	25%	$\gamma\ K^+K^-$	spin analysis (mi)
Mark-III [122] , DM2 [64]	yes	no	$\varphi\ K^+K^-$	interference
(2) central production :				
WA76 [123]	yes	no	$p\ K\overline{K}\ p$	spin analysis (sb)
E690 [124]	yes	yes	$p\ K_sK_s\ p$	spin analysis (mi)
(3) peripheral production :				
BNL [84]	no	yes	$n\ K_sK_s$	spin analysis (mi)

Table 15. Properties of the basic triplet of binary glueballs gb

name	PDG	mass (MeV)	mass^2(GeV)^2	width (MeV)
gb (0^{++})	$f_0(400-1200)$	~ 1000	$\sim 1.$	$500-1000$
	$f_0(1300)$			
gb (0^{-+})	$\eta(1440)$	$1400\ -\ 1470$	2.07	$50\ -\ 80$
gb (2^{++})	$f_J(1710)$	$1712\ \pm\ 5$	2.93	$133\ \pm\ 14$

The support for this assignment comes from the Gell-Mann-Okubo mass formula (after rejecting the $K\overline{K}$ bound state interpretation of $a_0(980)$), the $J/\psi \to \phi/\omega + f_0(980)$ decays, the branching ratios for decays of the scalars into pairs of pseudoscalars as well as the amplitude signs we obtained. The most important information comes from phase shift analyses of elastic and inelastic $\pi\pi$ scattering as well as from the recent analyses of $p\overline{p}$ annihilation near threshold.

2. *The* 0^{++} *glueball of lowest mass*
The broad object which extends in mass from 400 MeV up to about 1700 MeV is taken as the lightest 0^{++} glueball. In this energy range, the $\pi\pi$ amplitude describes a full loop in the Argand diagram after the $f_0(980)$ and $f_0(1500)$ states are subtracted. In particular, we do not consider the occasionally suggested $\sigma(700)$ and the $f_0(1370)$, listed by the Particle Data Group as genuine resonances, since the related phase movements are too small.
This hypothesis is further supported by the occurrence of this state in most reactions which provide the gluon-rich environment favorable for glueball production, also by the decay properties in the 1300 MeV region and especially by the strong suppression in $\gamma\gamma$ collisions. An exception is perhaps the decay $J/\psi \to \pi\pi\gamma$, but no complete amplitude analysis is available yet in this case.

3. *The* 0^{-+} *and* 2^{++} *glueballs.*
The triplet of binary glueballs is completed by the state $f_J(1710)$, for which by now overwhelming evidence exists in favor of a dominant spin 2 component, and the 0^{-+} state $\eta(1440)$. They appear with large branching ratios in the radiative decays of the J/ψ, in agreement with the expectations for a glueball. Central production in pp collisions is observed for $f_2(1710)$, but less significantly for $\eta(1440)$, so this assignment is at a more tentative level.

The properties of the basic triplet of binary glueballs are summarized in Table 15. Interestingly, the mass square of these states are separated by about 1 GeV^2 as in case of the $q\overline{q}$ Regge recurrences.

Whereas this overall picture of the low-mass $q\overline{q}$ and gg states seems to accommodate the relevant experimental facts, there is certainly a need for further improvements of the experimental evidence, for which we give a few examples:

1. *Elastic and inelastic* $\pi\pi$ *scattering*
The status of elastic $\pi\pi$ scattering above 1.2 GeV is still not satisfactory. The phase shift analysis of available $\pi^0\pi^0$ data could be of valuable help to establish the parameters of the $f_0(1500)$ in this channel and to determine the behaviour of the "background" amplitude, the same applies for the $\eta\eta$ channel. It will be

interesting to obtain a decomposition of the "background" from $f_0(980)$ and find the relative signs of the components.

2. *Branching ratios of scalar mesons*
Of particular interest are the tests of predictions on the decays $J/\psi \to \phi/\omega + f_0(1500)$ to further establish the quark composition of this state. The same applies for the 2γ widths of both isoscalar states.
3. *Production and decay of the lightest glueball*
The radiative decays of the J/ψ into $\pi\pi$ and other pseudoscalars are naturally expected to show a signal from the lightest glueball. So far, the experimental results have been plagued by background problems and the dominance of higher spin states like $f_2(1270)$; a spin analysis is required to get more clarity. The decays of this object into other pseudoscalars above 1 GeV is of interest.
4. *Glueballs in $\gamma\gamma$ collisions*
If the mixing with $q\overline{q}$ is small, the production of the glueballs should be suppressed. For the lightest glueball this is observed in the mass region below 1 GeV. It is of crucial importance to demonstrate this suppression in the region above 1 GeV in the 0^{++} wave. Here, only $f_0(980)$ and the $f_0(1500)$ should remain as dominant features.

Our hypotheses on the spectroscopy of low-lying glueballs and $q\overline{q}$ states are not in contradiction with theoretical expectations. The masses in Table 15 are in good agreement with the expectations from the bag model. Also the QCD sum rules suggest a strong gluonic coupling of 0^{++} states around 1 GeV. It will be interesting to see whether the more complete lattice calculations now on their way yield a "light" gluonic 0^{++} state around 1 GeV as well as "light" scalar $q\overline{q}$ mesons. It is expected that a light glueball is much broader than the heavier brothers, and this is consistent with our scheme in Table 15.

We found the most general effective potential for the scalar nonet sigma variables to be compatible with the $a_0 - f_0$ mass degeneracy, independently of the strange quark mass m_s. The mass splitting $O(m_s)$ shows a continuum of breaking patterns not necessarily along the OZI rule, as often assumed from the beginning. It remains an open question in this approach, though, what the physical origin of the $a_0 - f_0$ mass degeneracy is and the same holds for the mirror symmetry of the mixing patterns in the scalar and pseudoscalar nonets. A possible explanation for the latter structure is suggested by a renormalizable model with an instanton induced $U_A(1)$-breaking interaction.

References

1. H. Fritzsch, P. Minkowski, Nuovo Cim. **30A** (1975) 393
2. F.E. Close, Rep. Prog. Phys. **51** (1988) 833
3. C.A. Heusch, Proc. QCD – 20 years later. Aachen, June 1992, Eds. P.M. Zerwas, H.A. Kastrup (World Scientific, Singapore, 1993), p. 555
4. C. Michael, Proc. NATO Advanced Study Inst. Confinement, Duality and Nonperturbative Aspects of QCD. Cambridge, June 1997, Ed. P. van Baal, NATO ASI Series B: Physics Vol. 368 (1998) 1
5. M. Teper, Proc. NATO Advanced Study Inst. Confinement, Duality and Nonperturbative Aspects of QCD. op. cit. p.43
6. Crystal Barrel Coll., C. Amsler et al., Phys. Lett. B **342** (1995) 433; V.V. Anisovich et al., Phys. Lett. B **323** (1994) 233
7. C. Amsler et al., Phys. Lett. B **333** (1994) 277
8. C. Amsler et al., Phys. Lett. B **291** (1992) 247
9. C. Amsler et al., Phys. Lett. B **340** (1994) 259
10. C. Amsler et al., Phys. Lett. B **353** (1995) 571
11. Crystal Barrel Coll., A. Abele et al., Phys. Lett. B **380** (1996) 453
12. WA102 Coll., D. Barberis et al., Phys. Lett. B **397** (1997) 339
13. D. Barberis et al., Phys. Lett. B **413** (1997) 225
14. R. Landua, Proc. 28th Int. Conf. on High Energy Physics, Warsaw, July 1996, Eds. Z. Ajduk, A.K. Wroblewski (World Scientific, Singapore, 1997), p.1
15. C. Amsler, F.E. Close, Phys. Rev. D **53** (1996) 295; Phys. Lett. B **353** (1995) 385
16. V. V. Anisovich, Yu. D. Prokoshkin , A. V. Sarantsev, Phys. Lett. B **389** (1996) 388; V. V. Anisovich , A. V. Sarantsev, Phys. Lett. B **382** (1996) 429
17. F.E. Close, Proc. DAPHNE workshop on Hadron Dynamics, Frascati, Italy, Nov. 1996, Nucl. Phys. A **623** (1997) 125c
18. Particle Data Group, C. Caso et al., Eur. Phys. J. C **3** (1998) 1, (http://pdg.lbl.gov/)
19. R.L.Jaffe, K. Johnson, Phys. Lett. **60B** (1976) 201
20. T. Barnes, F.E. Close, S. Monaghan, Nucl. Phys. B **198** (1982) 380
21. M.A. Shifman, A.I. Vainshtein, V.I. Zakharov, Nucl. Phys. B **147** (1979) 385,448
22. S. Narison, Nucl. Phys. B **509** (1998) 312; Nucl. Phys. B (Proc. Suppl.) **64** (1998) 210
23. E. Bagan, T.G. Steele, Phys. Lett. B **243** (1990) 413
24. P. De Forcrand et al., Phys. Lett. B **152** (1985) 107; C. Michael, M. Teper, Nucl. Phys. B **314** (1989) 347; G. S. Bali, A. Hulsebos, A. C. Irving, C. Michael, K. Schilling, P. Stephenson, Phys. Lett. B **309** (1993) 378; H. Chen, J. Sexton, A. Vaccarino, D. Weingarten, Nucl. Phys. B (Proc. Suppl.) **34** (1994) 357
25. D. Weingarten, Nucl. Phys. B (Proc. Suppl.) **53** (1997) 232
26. C.J. Morningstar, M. Peardon, Phys. Rev. D **56** (1997) 4043
27. G. S. Bali et al. (SESAM Coll.), Nucl. Phys. B (Proc. Suppl.) **53** (1997) 239
28. G. S. Bali et al. (SESAM and TχL Coll.), Nucl. Phys. B (Proc. Suppl.) **63** (1998) 209
29. M. Göckeler et al., Phys. Rev. D **57** (1998) 5562
30. J. Weinstein, N. Isgur, Phys. Rev. Lett. **48** (1982) 659; Phys. Rev. D **27** (1983) 588; R. Jaffe, Phys. Rev. D **15** (1977) 267
31. B.W. Lee, Chiral Dynamics. Gordon and Breach (New York, 1972); T.Hatsuda, T. Kunihiro, Phys. Rep. **247** (1994) 223; R. Alkofer, H. Reinhardt, Chiral Quark Dynamics. Springer (Berlin, Heidelberg 1995)
32. N. A. Törnqvist, preprint The linear U(3)xU(3) Sigma Model, the $\sigma(500)$ and the Spontaneous Breaking of Symmetries. hep-ph/9711483; see also Z. Phys. C **68** (1995) 647

33. V. Dmitrašinović, Phys. Rev. C **53** (1996) 1383
34. E. Klempt, B.C. Metsch, C.R. Münz, H.R. Petry, Phys. Lett. B **361** (1995) 160
35. L. Burakovsky, T. Goldmann, Nucl. Phys. A **628** (1998) 87
36. G. t' Hooft, Phys. Rev. D **14** (1976) 3432
37. P. Minkowski, Nucl. Phys. (Proc. Suppl.) **7A** (1989) 118
38. J. Bijnens, Int. J. Mod. Phys. A **18** (1993) 3045
39. B. Hyams et al., Nucl. Phys. **64B** (1973) 4; W. Ochs, Ludwig-Maximilians-University Munich, thesis 1973 (unpublished)
40. G. Grayer et al., Nucl. Phys. **75B** (1974) 189
41. K. L. Au, D. Morgan, M. R. Pennington, Phys. Rev. D **35** (1987) 1633
42. D. Morgan, M. R. Pennington, Phys. Rev. D **48** (1993) 1185
43. S. J. Lindenbaum, R. S. Longacre, Phys. Lett. B **274** (1992) 492
44. D.V. Bugg, A.V. Sarantsev, B.S. Zou, Nucl. Phys. B **471** (1996) 59
45. BNL – E852 Coll., J. Gunter et al., Analysis of the $\pi^0\pi^0$ final state in the $\pi^- p$ reactions at 18.3-GeV/c, hep-ex/9609010
46. B. R. Martin, D. Morgan, G. Shaw, Pion-Pion Interactions in Particle Physics (Academic Press, London, 1976)
47. W. Ochs, πN - Newsletter **3** (1991) 25
48. M. Alston-Garnjost et al., Phys. Lett. B **36** (1971) 152; S.D. Protopopescu et al., Phys. Rev. D **7** (1973) 1279 S.M. Flatté et al., Phys. Lett. **38B** (1972) 232
49. W.D. Apel et al., Phys. Lett. **41B** (1972) 542
50. P. Estabrooks, A.D. Martin, $\pi\pi$ scattering – 1973, A.I.P. Conf. Proc. 13, Eds. P.K. Williams, V. Hagopian (American Inst. of Phys. New York, 1973), p. 37
51. CERN-Cracow-Munich Coll. H. Becker et al., Nucl. Phys. B **150** (1979) 301
52. CERN-Cracow-Munich Coll. H. Becker et al., Nucl. Phys. B **151** (1979) 46
53. M. Svec, Phys. Rev. D **55** (1997) 5727; M. Svec, preprint hep-ph/9607297
54. R. Kamiński, L. Lesńiak and K. Rybicki, Z. Phys. C **74** (1997) 79
55. GAMS Coll., D. Alde et al., Z. Phys. C **66** (1995) 375
56. W. Ochs, Nuov. Cim. **12A** (1972) 724; Proc. 2nd Int. Conf. on Nucleon-Nucleon Interactions, Vancouver, 1977 (American Institute of Physics, New York, 1978), p.326
57. C.D. Frogatt, D. Morgan, Phys. Lett **40B** (1972) 655
58. P.Estabrooks, A.D. Martin, Phys. Lett **41B** (1972) 350
59. W. Ochs, F. Wagner, Phys. Lett **44B** (1973) 271
60. P.Estabrooks, A.D. Martin, Nucl. Phys. B **79** (1974) 301; **95** (1975) 322
61. D.M. Binnie et al., Phys. Rev. Lett **31** (1973) 1534
62. E-760 Coll., T.A. Armstrong et al., Phys. Lett. B **307** (1993) 399
63. Mark II Coll., G. Gidal et al., Phys. Lett. **107B** (1981) 153
64. DM2 Coll., A. Falvard et al., Phys. Rev. D **38** (1988) 2706
65. Mark III Coll., W.S. Lockman, Proc. of the 3rd Int. Conf. on Hadron Spectroscopy, Ajaccio, France, Sept. 1989
66. DM2 Coll., J.E. Augustin et al., Nucl. Phys. B **320** (1989) 1
67. Crystal Ball Coll., H. Marsiske et al., Phys. Rev. D **41** (1990) 3324
68. Mark II Coll., J. Boyer et al., Phys. Rev. D **42** (1990) 1350
69. JADE Coll., T. Oest et al., Z. Phys. C **47** (1990) 343
70. AFS Coll., T. Akesson et al., Nucl. Phys. B **264** (1986) 154
71. GAMS Coll., D. Alde et al., Phys. Lett. B **397** (1997) 350
72. N.N. Achasov, G.N. Shestakov, Phys. Rev. D **58** (1998) 054011
73. M.P. Locher, V.E. Markushin, H.Q. Zheng, Eur. Phys. J. C **4** (1998) 317
74. OPAL Coll., K. Ackerstaff et al., Eur. Phys. J. C **4** (1998) 19
75. B. Hyams et al., Nucl. Phys. B **100** (1975) 205; W. Männer, 4th Int. Conf. on experimental meson spectroscopy, Boston, 1974 (AIP Conf. Proc. no. 21, particles and fields subseries no. 8) p.22
76. Omega Spectrometer Coll., M.J. Corden et al. Nucl. Phys. B **157** (1979) 250
77. E. Barrelet, Nuov. Cim. **8A** (1972) 331
78. T. Shimada, Prog. Theor. Phys. **54** (1975) 758
79. A.D. Martin, M.R. Pennington, Ann. Phys. (N.Y.) **114** (1978) 1
80. IHEP-NICE Coll., W.D. Apel et al., Nucl. Phys. B **201** (1982) 197
81. V. V. Anisovich, A. A. Kondashov, Yu. D. Prokoshkin, S. A. Sadovsky, A. V. Sarantsev, The two pion spectra for the reaction $\pi^- p \to \pi^0\pi^0 n$ at 38 GeV/c pion momentum and combined analysis of the GAMS, CRYSTAL BARREL and BNL data. hep-ph/9711319
82. Argonne Coll., D. Cohen et al., Phys. Rev. D **22** (1980) 2595
83. OMEGA Coll., G. Costa et al., Nucl. Phys. B **175** (1980) 402
84. BNL Coll., A. Etkin et al., Phys. Rev. D **25** (1982) 1786
85. CERN-Krakow-Munich Coll., L. Görlich et al., Nucl. Phys. B **174** (1980) 16
86. IHEP-IISN-LAPP Coll., F. Binon et al., Nuov. Cim. **78A** (1983) 313
87. IHEP-IISN-LAPP Coll., F. Binon et al., Nuov. Cim. **80A** (1984) 363
88. IHEP-IISN-LANL-LAPP Coll., D.Alde et al., Nucl. Phys. B **269** (1986) 485
89. C. Amsler et al., Phys. Lett. B **355** (1995) 425
90. E-760 Coll., T.A. Armstrong et al., Phys. Lett. B **307** (1993) 394
91. C. Zemach, Phys. Rev. B **140** (1965) 97, 109
92. V.V. Anisovich, A.V. Sarantsev, Phys. Lett. B **382** (1996) 429
93. C. Amsler, Rev. Mod. Phys. **70** (1998) 1293
94. V. Bugg, V.V. Anisovich, A. Sarantsev, B. S. Zou, Phys. Rev. D **50** (1994) 4412
95. M. J. Corden et al., Nucl. Phys. B **144** (1978) 253
96. C. Defoix et al., Nucl. Phys. B **44** (1972) 125
97. ALEPH Coll., Contribution to ICHEP98 Conference, Vancouver, July 1998, Abstract number 907
98. Crystal Ball Coll., C. Edwards et al., Phys. Rev. D **25** (1982) 3065
99. R.A. Lee, PhD thesis, Stanford University, SLAC-Report 282, 1985 (unpublished)
100. C. Edwards et al., Phys. Rev. Lett. **48** (1982) 458
101. Mark III Coll., R.M. Baltrusaitis et al., Phys. Rev. D **35** (1987) 2077
102. Aaron et al., Phys. Rev. D **24** (1981) 1207
103. D. Morgan, M.R. Pennington, Z. Phys. C **48** (1990) 623
104. G. Veneziano, Nuovo Cim. **57A** (1968) 190

105. D. Iagolnitzer, J. Zinn-Justin, J.B. Zuber, Nucl. Phys. B **60** (1973) 233
106. B.S. Zou, D.V. Bugg, Phys. Rev. D **50** (1994) 591
107. P.G.O. Freund, Phys. Rev. Lett. **20** (1968) 235; H. Harari, ibid., p. 1395
108. C. Quigg, 4th Int. Conf. on experimental meson spectroscopy, [75], p. 297
109. MarkII Coll., D.L. Scharre et al., Phys. Lett. B **79** (1980) 329
110. Crystal Ball Coll., C. Edwards et al., Phys. Rev. Lett. **49** (1982) 259
111. Mark-III Coll., T. Bolton et al., Phys. Rev. Lett. **69** (1992) 1328
112. DM2 Coll., J.E. Augustin et al., Phys. Rev. D **46** (1992) 1951
113. WA76 Coll., T.A. Armstrong et al., Z. Phys. C **56** (1992) 29
114. M. Chanowitz, Phys. Rev. Lett. **46** (1981) 981
115. J.E. Augustin et al., Z. Phys. C **36** (1987) 369
116. J.E. Augustin et al., Phys. Rev. Lett. **60** (1988) 2238
117. T. Bolton, Ph.D. thesis (MIT) 1988, unpublished
118. L.P. Chen, Ph.D. thesis (UMI-92-30905-mc) 1991, unpublished
119. Mark-III Coll., L.P. Chen et al., Nucl. Phys. (Proc.Suppl.) **21** (1991) 80
120. Mark-III Coll., L.P. Chen et al., Proc. Hadron '91, College Park, Maryland, Aug. 1991, SLAC-PUB-5669 (Oct. 1991)
121. J.Z. Bai, Phys. Rev. Lett. **77** (1996) 3959
122. L. Köpke (representing the Mark-III Coll.), in Strong Interactions and Gauge Theories. 21. Rencontres de Moriond, Les Arcs, France, March 16-22, 1986, , Ed. J. Tran Than Van, (Editions Frontières, Gif sur Yvette, France, 1987), p. 437
123. WA76 Coll., T.A. Armstrong et al., Phys. Lett. B **227** (1989) 186
124. E690 Coll., M.A.Reyes et al., Phys. Rev. Lett. **81** (1998) 4079